Selection of thermal management system for modular battery packs of electric vehicles: A review of existing and emerging technologies

1 author:

Shashank Arora
Aalto University
28 PUBLICATIONS   **283** CITATIONS

Title: Selection of Thermal Management System for Modular Battery Packs of Electric Vehicles: A Review of Existing and Emerging Technologies

Shashank Arora*

Faculty of Science, Engineering and Technology

Swinburne University of Technology

Hawthorn, Victoria, 3122, Australia

* Corresponding author:

Tel.: +358504351511;

E-mail: shashankarora@outlook.com.au

Abstract

Li-ion battery cells are temperature sensitive devices. Their performance and cycle life are compromised under extreme ambient environment. Efficient regulation of cell temperature is, therefore, a pre-requisite for safe and reliable battery operation. In addition, modularity-in-design of battery packs is required to offset high manufacturing costs of electric vehicles (EVs). However, modularity of battery packs is restricted by flexibility of traditionally used battery thermal management systems. For example, scalability of liquid cooled battery packs is limited by plumbing or piping and the auxiliary equipment used in the system. An alternative thermal management system is, therefore, required for modular EV battery packs.

In this paper, state-of-the-art developed to control battery temperature near a pre-specified state is qualitatively reviewed with the intent to identify potential candidate for implementation in a modular architecture. Some of the novel techniques that provide high-scalability in addition to appreciable cost and energy-savings over traditional methods are also evaluated while considering the development state and associated technical risks. It is found that only a hybrid system can meet technical requirements imposed by modular design. Based on the current state, phase change materials and thermoelectric devices are more likely to be part of this next generation thermal management system.

Keywords:

1. Introduction

Various chemical reactions and electrochemical transport phenomena characterise the normal charging and discharging processes in a battery cell. Many of these reactions are exothermic in nature [1], meaning that temperature affects the performance of a battery pack. General Motors estimated that if an electric vehicle (EV) is operating in sub-zero temperatures, its driving range can be reduced by several percent due to the sluggish charge kinetics in the battery cells [2]. On the other hand, if heat transfer from the battery pack to the external environment is not sufficient, excess heat may accumulate in the battery pack, particularly when it is being operated in a hot climate or under an insulating environment [3]. Hot spots can also develop, leading to an uneven temperature distribution across the battery pack, which can alter charging and discharging characteristics of the battery cells [4, 5]. More importantly, the battery cell temperature may rise beyond the safety limits of 60 °C for Li-ion battery cells using $LiBF_4$ as electrolyte, risking battery pack failure [6].

Previous studies indicate that the battery cell temperature must be regulated within a predefined operating range to sustain a rate of reaction considered healthy for the efficient operation of battery cells. The recommended operational range for Li-ion battery cells is generally between 25 °C and 40 °C [7, 8]. Managing large temperature spikes and non-uniform thermal gradients across the battery pack is, therefore, a major concern in the design of large battery packs essential for supporting an EV driveline. For these reasons, a battery thermal management system (TMS) needs to be integrated with the EV battery pack, although the original equipment manufacturers (OEMs) have followed different approaches [9]. **Table 1** separates the OEMs that are in favour of using a TMS from those who do not use it.

OEMs **not using** TMS	OEMs **using** TMS
Nissan	Tesla
BYD	General Motors
Volkswagen	Ford
Mitsubishi	Mercedes
Renault	Fiat

Table 1: List of OEMs distinguishing those which prefer to use a thermal management system for their EV battery packs from those which do not (*Mitsubishi iMiEV offers a variant with forced air-cooled battery pack, i.e. there is an optional fan that can be attached to its battery back for limiting the temperature rise during fast charging operations)

Several incidents involving battery cells overheating and catching fire have been reported to date. In many cases, the problem of battery overheating has caused OEMs to question the reliability of battery packs and loss of markets for battery-powered products. **A** list of major product recalls and incidents of battery-powered products catching fire in recent history is available from [10].

It is evident that thermal stability is a major issue for Li-ion battery packs. In addition, the high manufacturing costs of battery packs hinder the marketability of EVs. Mass market appeal of EVs can be improved by using economies of scale generated by the implementation of modular battery pack architecture. However, the concepts of mechanical and thermal modularity are inter-connected. The thermal independence of each battery cell must be ensured to preserve their interchangeability [11]. In this paper, different thermal management techniques that can be applied for the regulation of the thermal behaviour of Li-ion battery packs are qualitatively reviewed to ascertain their suitability for potential implementation in a modular system. In order to provide more context for this work, the paper first presents a simplified overview of the main issues affecting behaviour of the Li-ion battery cells in low/elevated ambient temperatures.

2. Effect of temperature on Li-ion battery cells

Li-ion battery cells belong to a category of temperature-sensitive devices, since both their performance and their safety are influenced by their operating temperature [12]. Research has shown that commercial Li-ion battery cells achieve optimum performance near room temperature [13]. This section discusses various challenges associated with operating Li-ion battery cells in temperatures that are far from this ideal condition.

2.1 Effect of low temperature

It has been reported that *18650* type Li-ion battery cells can supply only 5% and 1.25% of the energy capacity and power capacity available at 20 °C, respectively, in low operating temperatures such as -40 °C [14]. Similarly, the driving range of the 2012 Nissan LEAF has been noted to drop substantially from 138 miles in ideal conditions to 63 miles at -10 °C. Moreover, information presented by different research groups [14-16] on the energy capacity of Li-ion batteries available during constant current discharge/charge tests conducted in low temperatures confirms that the usable battery capacity decreases as the operating temperature is reduced.

It was previously believed that the unsatisfactory performance of Li-ion battery cells at low temperatures was due to their limited electrolyte conductivity, which affects the Li-ion transportation rate between the two electrodes at these temperatures. However, further investigations suggest that inadequate electrode activity can also cause poor low temperature performance in Li-ion battery cells. Electrode activity refers to the combined effect of marginalised Li-ion transfer through surface films on Li-ion battery cell electrodes called the solid electrolyte interphase (SEI), and the high charge-transfer resistance and slow diffusivity of Li-ions within the anode materials [17-21].

Of the control factors [22, 23], the choice of electrolyte for Li-ion cells is critical to the improvement of their low-temperature performance, primarily because of the intrinsic loss of ionic conductivity associated with low operating temperatures. In addition, SEI film's chemical composition and physical characteristics, such as its resistance and conformability to Li intercalation, depend on the salt forming the electrolyte, and parameters such as the quality of the anode material, and the mode and temperature of the SEI formation [24, 25]. SEI is a surface film approximately 5 Å to 800 Å thick, consisting of both organic and inorganic compounds, which keeps the electrolyte kinetically stable at anode potentials of less than 0.8 V. The thickness of the film varies with the degree of anode graphitisation [26, 27]. Interestingly, this anodic film is highly resistive and interferes with the Li-ion transport kinetics at the electrolyte/electrode interphase [28]. Most research activities to date have therefore focussed on improving the conductivity and stability of electrolytes with effective SEI film formation. Approaches that have been central to this improvement are:

1. Use of co-solvents with low viscosity and low freezing temperatures, such as glymes, esters and lactones [29-31]

2. Formulation of new additives for electrolytes to further lower their freezing point [32-35]

3. Substitution of the existing lithium salt $LiPF_6$ with new mixtures to improve the charge transfer resistance and other characteristics of the SEI film [36-40]

2.2 Effect of elevated temperatures

United States Advanced Battery Consortium (USABC) has defined a performance target of 15 years' calendar life for all the battery packs to be used in HEVs, while the targeted calendar life for EV battery packs is 10 years [41]. It is, therefore, of utmost concern that elevated temperatures, i.e. temperatures greater than 40 °C, accelerate the battery ageing phenomena. Battery ageing refers to the loss of the energy/power retention capacity of a battery as a function of time and inhibits battery packs from meeting the USABC performance goals.

Most electrolytic compounds are not chemically stable at voltage potentials that exists on the anode, i.e. the negative electrode of a Li-ion battery cell. When a new battery cell is charged for the first time, some of the electrolyte is irreversibly reduced by reacting with free Li-ions near the electrode/electrolyte interphase, forming a thin film of metastable lithium alkyl carbonates, polymers and gaseous products on the surface of the carbonaceous anode. This film is pervious to lithium cations but impervious to electrons and any other chemical species floating in the electrolyte. Electrolytic reduction therefore continues until a steady-state is reached where a surface film thick enough to block all the electrons from entry, covers the entire anode surface. It is commonly known as SEI film and prevents the electrolyte from corroding the charged anode due to chemical reduction with little effect on the Li-ion transportation rate through it [42, 43].

| Battery cell temperature	Cause	Leads to	Effect
High ↑	Electrolyte decomposition	Irreversible lithium loss	Capacity fade
	Continuous side reactions at low rate	Impedance Rise	Power fade
	Decrease of accessible anode surface for Li-ion intercalation		
	Decomposition of binder	Loss of mechanical stability	Capacity fade
25 °C – 40 °C	Maximum cycle life		
15 °C – 24 °C	Superior energy Storage capacity		
Low ↓	Lithium plating	Irreversible loss of lithium	Capacity/ power fade
	Electrolyte decomposition	Electrolyte loss	

Figure 1: Causes and effects of battery cell temperature on safety and performance

It has been reported that at elevated temperatures, impervious SEI film starts to break down and dissolve, leaving the anode surface exposed to electrolytic corrosion accompanied with the irreversible loss of lithium. SEI film dissolution also disturbs the physical equilibrium of the metastable organic components of SEI and initiates their transformation into a more stable inorganic form like lithium carbonate. The ionic conductivity or permeability of the SEI film gradually decreases as the percentage of inorganic carbonates in it starts to increase, marking a significant reduction in the energy capacity and power output of the battery cell [6, 44]. **Fig. 1** identifies the resulting effects of operating a battery cell at different temperatures and the causes leading to each failure mode.

The electro-chemical breakdown of the SEI film on the anode begins to happen around 85 °C and is the first step of a three-step process that leads to cell meltdown [45, 46]. If insufficient heat is removed from the battery cell at this stage, a point is reached where this process and the governing chemical reactions become self-sustaining. The battery cell then starts to self-heat at a rate greater than 0.2 °C/min and this is classified as thermal runaway [10, 47]. The second phase of the cell meltdown process is initiated when the battery cell temperature becomes greater than 140 °C. This marks the start of exothermic activity at the cathode, i.e. the positive electrode. Oxygen is rapidly released at the cathode and the battery cell now starts to self-heat at approximately 5 °C/min. The process finishes with oxidisation of the electrolyte as the cathode decomposes when the temperature reaches more than 180 °C. Self-heating rates around 11 °C/min have been cited for this phase, but they can increase up to 100 °C/min [48, 49]. The process is schematically described in **Fig. 2**.

The onset temperature for the exothermic reactions driving thermal runaway varies with the chemistry of the battery cells and their state of charge. In general, the higher the cell voltage or the state of charge, the lower the onset temperature for thermal runaway. For battery cells with the same chemistry, it varies with the load history of the specific cell and the abuse event [12].
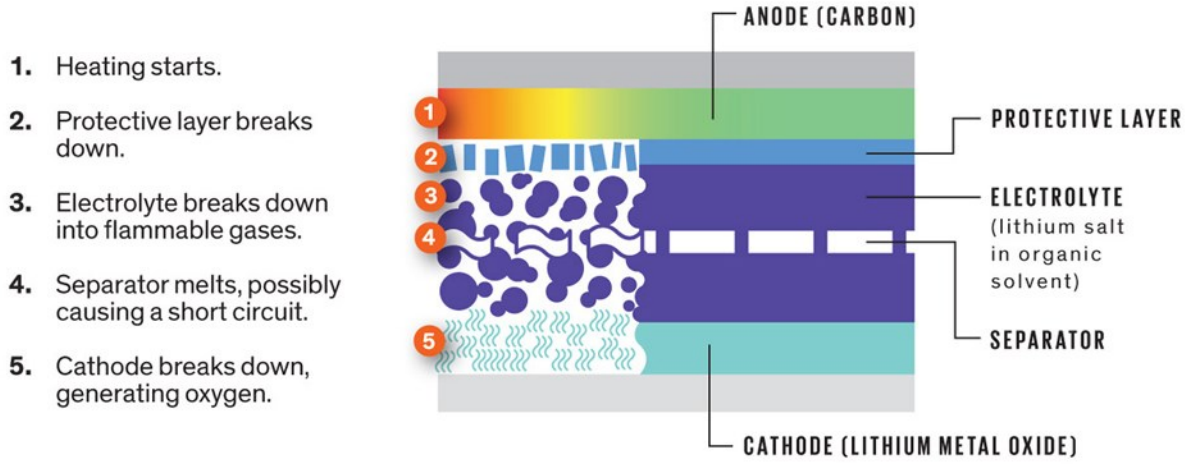
Figure 2: Illustration of thermal runaway process in Li-ion battery cells [50]

Research into electrolyte morphology indicates that $LiPF_6$ electrolyte solutions are characterised by increased decomposition at elevated temperatures [51]. It has also been reported that replacing cathode materials like $LiNiO_2$ and $LiNi_{0.8}Co_{0.2}O_2$ with $LiFePO_4$ or $Li[Ni_{3/8}Co_{1/4}Mn_{3/8}]O_2$ [52], or coating the surface of $LiCoO_2$ cathodes with Li_2ZrO_3 by a synchronised lithiation method [53], results in a thermally-stable cell. These positive discoveries have kept the research community motivated in their quest for stable electrolytes and safer cathode materials to improve performance at elevated temperatures. However, an appropriate thermal management strategy may provide additional safety by limiting the rate of heat accumulation inside the pack and pushing it to the state of thermal runaway.

3. Thermal Management Techniques

In this section, techniques developed to regulate the battery cell temperature near the pre-specified operating temperature are discussed. The first part presents methods that are exclusively applied for heating the battery cells. These are mainly used in extremely low ambient temperatures and are based on different strategies: internal heating, convective heating and pulse heating. Subsequently, more conventional battery thermal management methods are reviewed with the intent to select a TMS for modular battery packs. These methods are used

for managing irregular thermal spikes and maintaining a uniform temperature distribution in the battery pack. Lastly, the suitability of some of the emerging TMSs is also reviewed for modular battery pack application.

3.1 Pre-heating Strategies

Ji and Wang [54] recommend pre-heating battery cells to room temperature before normal operation in sub-zero temperature environments. They attribute the sluggish Li-ion kinetics in battery cells to the large change in their impedance at sub-zero temperatures. It has been noticed that at temperatures such as -20 °C the impedance levels can increase by approximately 10 times their value at room temperature and up to 20 times at -30 °C, marking a significant reduction in available energy and power from a Li-ion battery pack [21, 55]. High impedance accounts for large Ohmic heat generation and may induce a notable rise in battery cell temperature and restore the original performance index. The key is to appreciate the strong relationship between the thermal and electrochemical interactions in the Li-ion cells at sub-zero temperatures.

It is noteworthy that the energy balance between the electrochemical heat generation inside the battery, given by Equation 1 below, and the heat dissipated to the surroundings defines the battery cell temperature profile, which in turn regulates the temperature-dependent electrochemical processes inside the cell. A good understanding of the constantly-shifting equilibrium between heat generation and heat dissipation is fundamental to the development of heating techniques for Li-ion battery cells operating in sub-zero temperatures.

$$q = -IV - \sum_l I_l T^2 \frac{d\frac{U_{l,avg}}{T}}{dT} + \sum_j \frac{d}{dt}\left[\int_{v_j}\sum_i c_{i,j} RT^2 \frac{\partial}{\partial T}\ln\left(\frac{\gamma_{i,j}}{\gamma_{i,j}^{avg}}\right)dv_j\right] + \sum_{j,j\neq m}\sum_i\left[\left(\Delta H_{i,j\to m}^o - RT^2\frac{d}{dT}\ln\frac{\gamma_{i,m}^{avg}}{\gamma_{i,j}^{avg}}\right)\frac{dn_{i,j}}{dt}\right] \quad [1]$$

This principle has been utilised by Toyota and a system that uses the internal resistance of the battery to increase its temperature during vehicle operation was disclosed in US patent 6163135. In the design, battery temperature was closely monitored by temperature sensors. As the temperature falls below a predetermined level, a central processing unit performs a controlled charge or discharge of the battery to bring its temperature back up to the required level. The design exploits the basic quality of electrical machines to function as a simple load during the battery-discharge phase, and as a prime mover or generator if operated in reverse, i.e. the charging process. However, the system works only when the vehicle is switched on [56].

The limitation of this system was overcome by the design disclosed in US patent 7154068. The design includes a heater carefully placed between the top and the bottom layer of cells in the battery pack which can be regulated via the vehicle system controller. The heater is a positive temperature coefficient element the resistance of which to current flow increases as the ambient temperature decreases. In addition, the heat generated by it is directly proportional to the current flowing through it. An advantage of this heating mechanism is that it is battery-driven and therefore does not require any power cord to be plugged into an external power distribution system. Furthermore, the vehicle controller switches off the heater if the battery SOC falls below a pre-set value or the vehicle has/has not been in use for a long time to save energy. This feature is a big advantage when operating an EV in remote locations where distribution boxes might not be readily available [57].

Another way of improving the low temperature performance of a battery pack based on the fluid heating strategy is disclosed in US patent 7264902. The intent of this design is to provide a system that enables rapid heating of the battery pack, especially during the start-up phase, and to permit strict control over the battery cell temperature. Therefore, one or more good heat conductors with heating medium flowing in them are arranged adjacent to each battery cell.

This ensures that heat transfer through conduction from the heating system to the battery cells is not affected by the presence of any other medium between them. Each cell is formed in a thin plate shape to further enhance the heat conduction rate in the system. Moreover, the liquid electrolyte in the battery cells is replaced with a solid electrolyte. The replacement allows the reduction of the liquid seals used in the pack, thereby minimising its effective heat capacity. This design allows rapid heating and cooling of the battery pack [58].

Pesaran and co-workers compared the various preheating strategies using the finite element modelling technique. The problem was modelled as a pure heat-transfer phenomenon and the non-linearity introduced due to the complex electrochemical-thermal coupling in a battery pack was ignored. The evolution of battery cell temperature as a function of used energy capacity was then studied. Both the studies found core heating to be the most energy-efficient preheating method. Furthermore, only alternating current (AC) signals should be employed, as direct current (DC) pulses can cause damage to the battery core [59, 60]. In addition, Stuart and Hande experimentally analysed the possibility of using AC signals of different amplitudes for the external preheating of battery packs. In their investigation, lead acid batteries and nickel metal hydride batteries were exposed to AC signals of frequencies of 60 Hz and 20 kHz, respectively. It was observed that the speed of heating increases as the amplitude of the AC signal is increased [61].

While several pre-heating techniques for EV battery packs have been proposed, the selection of the most suitable strategy should be done only after ascertaining the cost and effect of heating time on the usable battery capacity and the cycle life of the battery pack.

3.2. Conventional temperature control methods

In recent years, a number of techniques for readily removing heat from a battery pack have been tried and tested by various research groups across the globe. They can be classified in various ways, as seen in **Fig. 3**. A brief explanation is provided in the following text.

Medium used: A battery thermal management system can be differentiated by the working fluid used in the cooling loop. They can be:

    A. Air-cooled: unidirectional or reciprocating

    B. Liquid cooled: Battery cells can be submerged directly in a di-electric working fluid. Alternatively, a separate piping could be used for regulating liquid flow around the cells. The piping could be in the form of:

        a. Jacketed cooling system
        b. Cold plates
        c. Heat pipes

    C. Phase change materials

    D. Any combination of the above

Power consumed: As per the standard definition, a TMS is considered an active system if it includes any power-consuming equipment, such as evaporators, blowers or pumps in the cooling loop; otherwise, it is classified as a passive system. In practice though, an active TMS is defined to be the one in which the cooling rate is controlled actively - for instance, the power-consuming equipment is turned on and off under pre-specified conditions. In addition, TMSs use a working fluid or coolant that absorbs excess heat and transfers it out of the system. This heat can be absorbed either as sensible heat, thus raising the temperature of the working fluid, or as latent heat, which causes it to undergo phase transformation. In general, all active systems remove heat as sensible heat of the fluid, while passive systems remove it as a latent heat.

Arrangement: Refers to the method of distributing working fluid within the battery pack

    A. External – Internal
    B. Series - Parallel
    C. Direct - Indirect
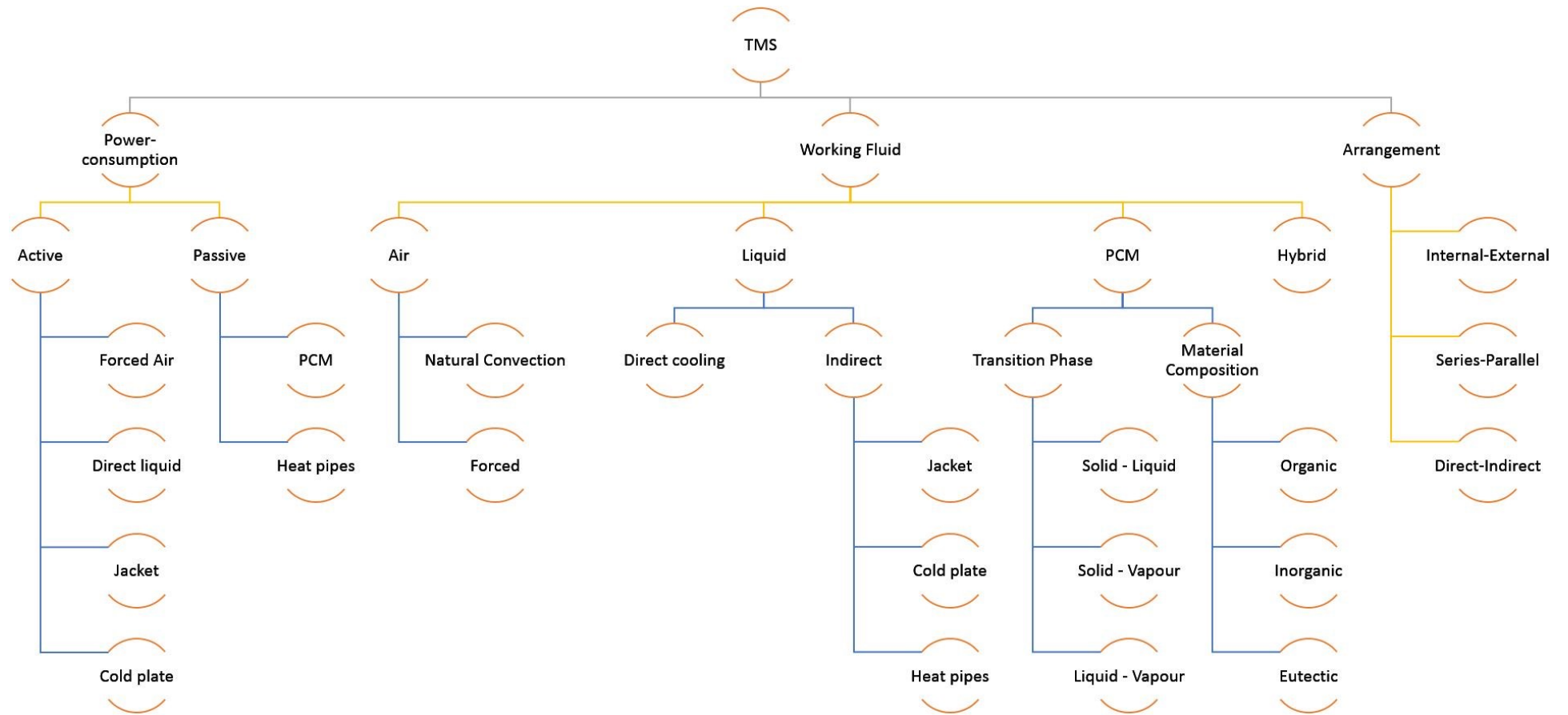
Figure 3: Classification of different battery thermal management techniques

3.2.1. Air-cooling

Blowing air through a fan [62] or from a wind tunnel [63] over a battery cell is probably the simplest and most cost-effective way of regulating its temperature. It has therefore garnered interest from several OEMs as a prospective thermal management solution for commercial EV battery packs. Many research activities have also been initiated mainly to consider the battery layout and optimise the airflow or the wind speed around it, and minimise the energy consumption and cost accrued. For instance, Xu and He [64] investigated different battery layouts and illustrated that arranging the batteries horizontally rather than longitudinally shortens the airflow path, thereby enhancing the heat dissipation characteristics of an air-cooled battery pack. Their experiments also proved that a double U-type duct can readily satisfy the heat dissipation requirements under a variety of environmental conditions, discharging/charging rates, or SOCs.

Fan et al. numerically studied the transient effect of airflow rate and gap spacing on the performance of an air-cooled battery pack made of eight evenly-spaced 15 Ah lithium manganese oxide pouch cells. The Li-ion battery pack was subjected to an aggressive driving test profile represented by the US06 profile scaled by a factor of 1.3. They reported that for a fixed flow rate of $20.4 m^3/h$, an improvement of 0.41 °C in the temperature uniformity within the battery pack was observed as the gap spacing increased from 1 mm to 5 mm. In addition, for a fixed spacing of 3 mm, the maximum temperature rise measured in the pack decreased by 1.8 °C when the flow-rate in an air-cooled battery was doubled from $20.4\ m^3/h$ to $40.8\ m^3/h$ [65].

In another study, Park numerically modelled the effect of an air flow manifold design for a particular battery layout (37 coolant passages 3 mm in diameter formed between 72 battery cells divided equally into 2 rows). Five configurations were studied: rectangular-shaped,

tapered manifolds (vertically contracting/expanding from 10 mm ↔ 20 mm), control design, and lastly, rectangular ventilation hole placed at the outlet of a tapered manifold. He observed that it was possible to achieve the desired cooling effect in an air-cooled pack by including pressure-relief ventilation and a tapered manifold in the wind/cooling tunnel. Further, a decrease from 47 W to 27 W in power consumption of fan was reported due to the presence of a tapered manifold with a ventilation hole [66]. Giuliano et al. studied metal-foam based air-cooled heat exchangers (HXs) for large-capacity lithium titanate battery packs. Their study confirmed that air-cooled HXs consume less power than liquid-cooled HXs and can be used effectively to regulate battery temperature in automotive applications [67].

While simple and sturdy in construction, air-cooled battery thermal management systems generally employ a unidirectional coolant flow in which ambient or conditioned air is admitted through one side of the battery pack and discharged from the opposite side. This is primarily the reason why air-cooled systems struggle to maintain a uniform thermal distribution and a gradient of less than 5 °C across a battery pack. This was confirmed by Lou, who designed a cinquefoil battery pack containing 5 modules in order to understand heat dissipation through an air-cooled Ni-MH battery pack. He noticed that although the maximum temperature was kept in check, the battery cells near the fan were operating at a lower cell temperature than those further away. In addition, the existence of a thermal gradient higher than 5 °C was confirmed for the battery pack [68].

US patent 7172831 illustrates that it is possible to overcome this basic limitation of air-cooled battery thermal management systems by using bi-directional or reciprocating airflow. The system makes use of a controller to actively operate the fan/pump, monitor that battery cell temperature and regulate the position of airflow valves. Active monitoring and control of the pump and flow passages cause the direction of the coolant flow to reverse after a pre-set

(optimised) time frame. As a result, the temperatures of battery cells on opposite sides of the pack averaged over time can be found to be approximately equal. It was further pointed out that the temperature difference between any two adjacent battery cells can be minimised by optimising the duration between the two successive flow reversals [69].

The authenticity of this claim has been verified by Mahamud and Park [62]. They numerically studied the effect of reciprocating airflow on the performance of an air-cooled battery pack made of $LiMn_2O_4/C$ cylindrical cells, using a lumped thermal capacitance model and a two-dimensional computational fluid dynamics model. The computational results were validated using an in-line tube bank set-up. It was found that a reciprocation period of 120 seconds can reduce the maximum cell temperature and temperature non-uniformity in the battery pack by 1.5 °C and 4 °C (equivalent to a 72% reduction), respectively, in comparison with the temperatures recorded for a battery pack with unidirectional air flow. Subsequently, He and Ma [70] developed an observer-based control strategy to regulate the amount of cooling flow required for reciprocating air flow systems. It was demonstrated that the cooling flow requirement for the reduction of the non-uniformity of thermal gradients existing in the battery back from 4.2 °C to 1 °C (i.e. by more than 76%), is decreased by 38% if the observer-based control strategy is used to regulate the air flow in reciprocating systems. In addition, He and co-workers [71] also developed a hysteresis controller that can reduce the parasitic power consumption of reciprocating air flow systems by 84%. However, the maximum cell temperature in this case was noted to be 17% greater than the instance when no control strategy was implemented.

3.2.2. Liquid Cooling

Studies have indicated that even extremely high air flow rates may not meet the heat dissipation requirements for an air-cooled EV battery pack that is being discharged or charged at an

aggressive rate in a hot ambient environment [72, 73]. Furthermore, the very low thermal conductivity of air may make it hard to cool a battery pack in a hot environment, thus compromising its safety. An alternative way of cooling a battery pack is by circulating a liquid coolant via jackets or through distinct tubes around it or placing it directly on a liquid-cooled plate. In a slightly different arrangement, battery modules can be submersed in a di-electric liquid such as de-ionised water or a silicon-based oil to increase the surface area available for heat dissipation. Such a thermal management system has been demonstrated by Pendergast et al., who placed a battery module with Panasonic 18650 cells arranged in an aluminium casing under water for cooling [74]. The higher heat capacity and thermal conductivity of traditional liquid coolants like water, acetone, glycol or oil make a liquid-cooled system more effective than an air-cooled system, despite the added mass, complexity and higher operating costs [75, 76]. It is estimated that using liquid cooled systems can be up to 3500 times more efficient than using air-cooled TMSs and lead to a reduction of up to 40% in parasitic load [77].

Nonetheless, not every liquid coolant may be as effective as others may for certain applications. For example, Kim and Pesaran found while experimenting with different coolants on cylindrical cells that water–ethylene glycol achieved superior cooling performance to mineral oil in an indirect liquid-cooled system. However, due to higher heat transfer coefficients in the case of a direct-contact cooling system, the performance of mineral oil was comparable to that of other coolants [78].

The previous section has described some examples of studies focussing on conventional liquid-cooled TMSs, which remove heat from a battery module via direct submersion or by circulating liquid in a jacket wrapped around the batteries. However, liquid-cooled systems can also be designed using cold plates and heat pipes, and these are described in the following sections.

a. Cold Plates

Cold plates are mostly preferred where strict space-limitations apply, such as in EV applications. They are basically thin-walled metal pressings with inbuilt channels for a liquid coolant to carry heat. In a liquid-cooled TMS with cold plates, metal pressings are generally arranged between adjacent battery cells and a liquid heat-transfer medium is pumped through the inbuilt channels. The liquid coolant then removes all the excess heat from the battery cells and transfers it to an external HX for dissipation to the ambient environment. The cooling performance of a cold plate is assessed in terms of the heat transfer rate, the thermal distribution across the pack, the power consumption depending upon the convective heat transfer coefficient between the plate and the liquid coolant, or the coolant flow rate and ambient temperature.

In the design of cold plates for EV battery packs, different channel designs and geometries may be required for different applications, whereas most current research models of cold plates are based on square-edged channel geometry. Furthermore, it can be concluded from the concurrent activities in relation to fuel cells that channel geometry is a critical parameter for cold plate design. In addition, the manufacture of square-edged channels is very expensive and sometimes impracticable [79]. This prompted Fisher and Torrance to deviate from square-edged channels and assess heat transfer through channels with rounded corners. They used the boundary element method to evaluate the performance of rectangular, diamond-shaped and elliptical channels. The results suggested that rectangular channels are more efficient than the other two configurations. Moreover, it was found that although more channels with elliptical design can be accommodated in the same packaging space, the heat transferred through a cold plate with elliptical channels is approximately 5% less than that transferred through a cold plate with rectangular channels [80, 81].

Studies by Yu et al. [82], Choi et al. [83] and Chen et al. [84] confirm that, in addition to the channel geometry, another parameter that can have a significant influence on the performance of a cold plate is the channel configuration, i.e. the route of coolant channels inside the metal pressing. Broad categories under which they can be grouped are: serpentine channels, parallel channels, and multi-channels. Jin et al. designed a thermal management system for EV battery packs using oblique fin cold plates. It was found that in cases of heating loads below 1240 W, this system could maintain the battery cell temperature to less than 50 °C with a flow rate lower than 0.9 l/min [85]. On the other hand, Jarrett and Kim employed cold plates with serpentine channels for the same purpose. Based on a CFD analysis, they discovered that channels of the greatest possible widths are necessary to achieve the lowest average temperature and minimum coolant pressure drop. In contrast, channels with a narrow inlet and gradually widening towards the outlet are required for maintaining thermal uniformity [79]. Huo et al. achieved the best cooling performance for a 5C discharge of a rectangular Li-ion battery cell by directing water into mini-channels on the sides of the electrode at a flow rate of $5x10^{-4}$ kg/s. However, they also observed an increased risk of failure at ambient temperatures higher than 25 °C and recommended a two-phase TMS for high-temperature applications [86]. Recently, Saw et al. proposed a two-phase TMS based on mist cooling or evaporative cooling for Li-ion battery packs [87]. Zareer et al. too confirmed superiority of ammonia boiling based TMS over a conventional single-phase liquid cooled system [88].
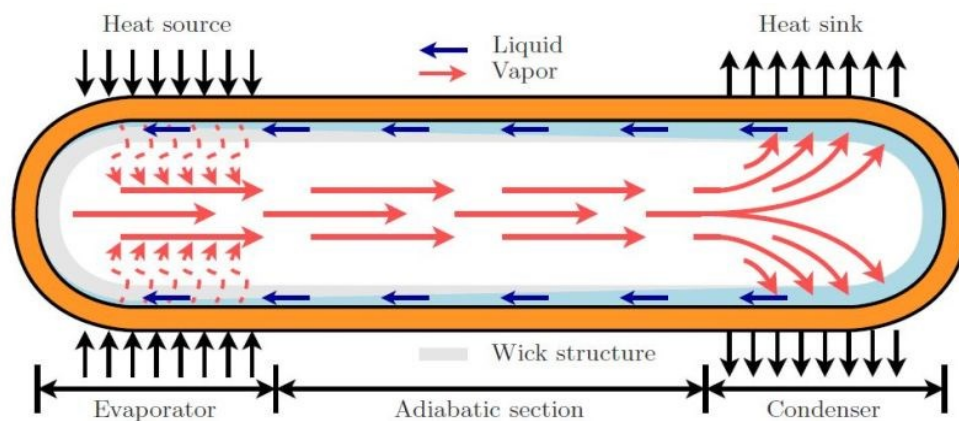
b.   Heat Pipes

A thermal management system with heat pipes is a passive system driven by capillary action of a wick material lining the internal surface of a vacuum-sealed shell. They have been in existence since 1942 when they were first introduced by R.S. Gaugler, and remove heat through the liquid-to-vapour phase change of a working liquid. Commonly used working fluids include water, acetone, methanol and ammonia but the choice of liquid for a specific system depends

upon the heat pipe shell material characteristics. E.g., both water and glycol/water solutions are compatible with copper shells; and in case of aluminium tubing, dielectric fluids and mineral oils can be used as working fluids in addition to water and glycol/water solutions. However, stainless-steel shells/channels are necessary if de-ionised water or any other corrosive media such as ammonia and acetone is the preferred working fluid for an application [89]. This applies to working fluid selection for cold plates as well.

A heat pipe can be usually divided into three parts, shown in **Fig. 4**:

1. Hot end or evaporating section

2. Adiabatic part or transport section

3. Cold end or condenser

Figure 4: Schematic of a traditional heat pipe with tubular structure and closed ends [90]

The liquid within the wick absorbs the excess heat from the battery cells, which are arranged towards the hot end of the heat pipe, and evaporates. The increased vapour pressure and reduced molecular density create a pressure gradient in the pipe that drives the hot vapours to the condensing section where heat is rejected to the HX. The capillary forces developed in the wick draw the condensed liquid back to the evaporator, thus completing the heat transfer cycle. It is noteworthy that since a vacuum exists in the heat pipe, the working fluid vaporizes at a temperature much below its normal boiling point, allowing the heat pipe to remove large

quantities of heat efficiently at much lower temperatures. Furthermore, the flexible geometry, low maintenance requirements and thermal conductivities that are twice the order of magnitude of solid conductors such as aluminium or copper, make them attractive as a TMS option for EVs.

Mahefkey et al. have designed a TMS incorporating heat pipes for Ni-Cd battery cells while Zhang et al. have done this for Ni-MH batteries. Both the groups found that heat pipes can mitigate any thermal excursions in the battery pack [91, 92]. Swanepoel investigated the possibility of using a pulsating heat pipe (PHP) with ammonia as the working fluid to regulate the battery cell temperature of Optima Spirocell lead-acid batteries. Based on experimental results and simulations, he discovered that a PHP with an internal diameter of less than 2.5 mm can successfully manage the thermal variations in the pack [93]. On the other hand, Wu et al. attempted to dissipate heat from a 12 Ah cylindrical Li-ion battery pack using two heat pipes with aluminium fins attached to their cold ends. Their experiments also confirmed that heat pipes can be used to keep battery cell temperatures in a safe range [94].

Various research groups have also tried to combine the benefits of heat pipes as a TMS with other cooling methods, in order to enhance the overall system performance. In one such trial, Jang and Rhi combined a loop thermo-siphon, which works on the same principle as a heat pipe, with forced air-cooling. In their experiments, they managed to control battery cell temperatures under 50 °C and 45 °C with pure water and acetone as coolants, respectively [95]. Rao et al. monitored the influence of cooling the condensing part of a heat pipe on its performance. They reported that the system could maintain the battery cell temperature under 50 °C as long as the heat generated by each cell was less than 50 W [96].

Vibrations ranging between 0 and 100 Hz can be transmitted to the battery pack in an EV from its top body. It is, therefore, imperative to analyse the influence of vibrations and shocks on the

performance of a heat pipe before defining it as fit-for-purpose in EVs. Connors and Zunner studied the behaviour of a flat heat pipe under vibrations. The heat pipe had an internal lining of copper powder to function as a wick material. They reported zero degradation in the cooling performance of a flat heat pipe when exposed to vehicle shock and vibration [97]. Similar conclusions could be drawn from the reports of Guo et al., who studied the effect of mechanical vibrations on the heat-dissipation abilities of rectangular grooves. They observed that the wetting area is enlarged by the vibrating motions of heat pipes. Vibrating motion also intensifies the heat transfer through the microgrooves, which enables the heat pipe to operate without any performance degradation in a vibrating environment [98].

So far, heat pipes have found limited usage in battery thermal management systems owing to the high capital costs incurred due to the application of copper as a wall and wick material, and the complicated fabrication process. However, recent advances in the manufacture of aluminium heat pipes promise substantial reductions in total system costs [99-102]. In addition, the weight savings realised by replacing heavier copper with lighter aluminum metal will benefit the EV sector.

3.2.2.1. Fouling/Scaling in tubular structure

Closed loops are used for recirculation of liquid coolant in the EV battery packs. The water-cooled systems are, thus, relatively less prone to biological fouling caused by exposure to light [103]. However, large heat generation during high C-rate operation of battery packs can also leave the wetted surface susceptible to scale formation if untreated water is used as a coolant. Liu et al. studied the effect of scale thickness on the heat transfer in axi-symmetric channels with water as coolant. Their work illustrated that heat transfer performance of channels covered with a 0.225 mm thick fouling layer is 5 times better than that of a channel with 1.55 mm thick fouling layer deposits [104].

Glycol/water solutions provide a greater resistance against biological fouling and scaling. It must be noted that although a higher glycol concentration leads to reduced thermal performance of the coolant, glycol concentrations less than 20% by volume have been found less effective in providing control over scale formation [105]. Adding graphene nanoplatelets into the mix is, therefore, recommended for improving the thermal performance of glycol solutions. Selvam et al. demonstrated that incorporating 0.5 vol% of graphene nanoplatelets in the glycol solution, increases thermal conductivity of water and ethylene glycol by 16% and 21%, respectively [106]. However, nanoplatelets can precipitate over time in the (micro)-channels. Sarafraz et al. demonstrated that a higher concentration of nanoparticles intensifies precipitation fouling regardless of the fluid velocity. Also, for all mass concentrations, fouling thermal resistance is defined by an inverse power function of Reynolds number [107].

Fouling of channels is partially responsible for high maintenance costs of liquid cooled systems. HX's surface vibrations are commonly used in the process industry to mitigate this issue. However, this technique is laborious and costly. Vibrations of the mechanical structure of the cooling system may affect integrity of adjoining battery cells as well. It is, therefore, not reliable. Pulsating working fluid, oscillating between 1Hz and ultrasonic frequencies, on the other hand, is a more practical approach. Research has shown that oscillating working fluid can not only reduce fouling but also increase heat transfer between the heat exchanging systems [108]. Tijing et al. also showed that a 16% to 60% reduction, depending on the frequency, in mineral fouling in HXs could be achieved using oscillating electric field [109].

3.2.3. Phase Change Materials

Traditional battery thermal management systems using forced-air cooling and liquid cooling are generally complex and bulky. They also add unavoidable electrical load in the form of fans, pumps, blowers, and HXs to the limited energy storage capacity of an EV. These undesirable disadvantages have increased the expectations for novel thermal management systems. A

simple passive solution comprising battery cells placed in a matrix of phase change materials with zero maintenance requirements has therefore been proposed as an alternative by a research group at the Illinois Institute of Technology. This solution employs the solid-liquid phase transformation of organic/inorganic/eutectic phase change materials (PCMs) to remove the thermal non-uniformities of the battery pack [110-112].

PCMs also have low maintenance requirements and have therefore piqued the interest of several research groups. For example, Khateeb et al. studied a Li-ion battery pack made of eighteen 18650 Li-ion cells and filled with a mixture of PCM and aluminium foam. They examined the thermal behaviour of this pack with the help of a numerical model that was validated through experiments at a later stage. It was also demonstrated through their experiments that the temperature rise in a battery pack can be reduced to half by using a TMS with PCM and aluminium foam, as opposed to the case where no TMS is applied [113]. Mills et al. simulated a laptop battery pack with six 2.2 Ah Li-ion cells and realised a uniform thermal distribution after using expanded graphite saturated with PCM as the thermal management solution [114]. Sabbah et al. compared the performance of a TMS with PCM to that of an air-cooled system using numerical methods and experiments. They demonstrated that the former could keep the temperature of a Li-ion battery cell below 55 °C, even at a constant discharge rate of 6.67C [115]. Kizilel et al. experimented with PCM-filled high-energy Li-ion battery packs and achieved a uniform thermal distribution under both normal and abusive test conditions [116]. Rao et al. also tested eutectic PCMs for 8 Ah prismatic $LiFePO_4$ battery cells. The results of numerous experiments simulations indicate that PCMs may be a practical solution to the thermal issues affecting EV battery packs [117]. Li et al. analysed the effectiveness of a PCM-filled copper foam sandwich panel as a cooling system for prismatic power batteries. The tests reflected a lower surface temperature and a better thermal uniformity in the battery module after the integration of the PCM-filled panels [118]. Arora et al. also

demonstrated that the high capacity PCM (RT28HC) could maintain 20 Ah $LiFePO_4$ pouch cell in a near-isothermal state during a 3C discharge process [119].

The mechanical behaviour of the thermal management system is as important as its thermal performance for making a reliable automotive-grade solution. It is beneficial to have a system design with a higher heat absorption rate, but it also necessary to have the required strength and stability to withstand normal stresses during daily vehicle operation. With this in mind, Alrashdan et al. undertook a systematic study to characterise the effect of the thermo-mechanical properties of eutectic PCMs (paraffin wax/expanded graphite), such as tensile and compression strength and thermal conductivity, on the reliability of Li-ion battery packs. At low as well as room temperatures, improvements in the thermo-mechanical properties, including tensile strength, burst strength, compression strength, and thermal conductivity of the pack were noticed, while they decreased at elevated temperatures [120].

However, phase-change materials have relatively low thermal conductivities. Consequently, they have slower regeneration times and cannot be effective in applications that may include fast charging followed by a quick discharge and then a fast charging of a battery pack in a short time. Several heat transfer enhancement techniques have been investigated for PCMs, which include the following:

1. The use of fixed and non-moving surfaces such as fins and honeycombs [121-125]
2. The employment of composite PCMs [126-128]
3. The impregnation of porous material [129-136]
4. The dispersion of high-conductivity particles in PCMs [137-141]

Table 2 summarises the research and development advancements made to the state-of-the-art of TMS since 2016.

Source/Research Method	Battery type	TMS	Design Parameters	Test Conditions	Key Findings
Huang et al. [142]/Experimental	5*6 - 1.1 Ah cylindrical cells connected in parallel	PCM + Liquid-cooling	Paraffin-EG matrix with embedded flat plate pipes; Pipe thermal conductivity = 10,000 W/m.K ; Cell spacing: 34mm (X-) and 25 mm (Z-direction) Coolant: ethyl alcohol	Ambient Temp: 35 °C ; Discharge rates of 1C, 2C and 3C; 5 cycles	▪ Inter-cellular temperature difference can be maintained below 3 °C by embedding flat pipes in PCM ▪ Liquid assisted PCM took longer to reach the maximum setting temperature of 44 °C in comparison to PCM with air-cooled pipes even at 3C discharge ▪ During cyclic discharge, liquid assisted PCM provided better control over max. battery temperature
Liang et al. [143]/ Experimental	Battery surrogate generating constant heat load	HP	Sintered Copper HP Evaporator section: 2mm thick; Outer dia: 6 mm; Horizontal working angle Working fluid: Water	Ambient Temp: 15 °C to 35 °C Flow rate: 2L/min	▪ Reducing coolant temperature can lead to constant HP performance in ambient temperatures between 25 and 35 °C ▪ Initial lag between starting times of battery and TMS is preferred in low ambient temperatures. In contrast, synchronized operation is beneficial in high ambient temperature cases.
Wu et al. [144]/ Experimental	Five 3.2V/ 12A prismatic cells connected in series	HP + PCM/EG + forced air-cooling	Sintered Copper – water HP; Width: 8mm; Thickness: 3mm; PCM/EG Melting point: 41.71 °C	Galvanostatic charge and discharge at rates between 1C and 5C; Air flow rate: 1 m/s to 4 m/s	▪ HP assisted PCM systems are found more effective than simple PCM system in case of repetitive cycling ▪ Initial and maximum temperatures of 32.9 °C and 55.7 °C are noted for HP-assisted PCM/EG system during cyclic use ▪ Air flow of 3 m/s caused a reduction of 5.2 °C in max. temperature
Ye et al. [145]/Experimental	16 LFP 18Ah prismatic cells joined in series	Micro-HP array	3mm-thick flat micro-HP array; 5° tilt angle; Heat pipe: 200 x 60 mm Fin: 20 x 24 x 1 mm	Room temperature: 27.56 °C; 1C charge and 3 min rest phase	▪ Intercellular gradient smaller than 5 °C noted in the pack installed with micro-HP array with fins
Wang et al. [146]/ Experimental	Aluminum block (115 x 90 mm) as	PCM + Oscillating HP	OHP: Copper capillary tube; Outer dia: 3mm and Inner dia: 1.8mm;	OHP Orientations: Horizontal, 45° tilt and vertical;	▪ For the same heating power, maximum temperature decreases with increasing OHP inclination angle

	battery surrogate		Working fluid: acetone; Paraffin melting point: 41 ±1 °C	Start-up temperature: 25 ±0.05 °C	▪ More uniform cell temperature distribution is achieved by placing cell terminals further away from adiabatic portion of OHP system ▪ Start-up temperature must be below PCM transition temperature
Hong et al. [147]/ Computational modeling	12 x 2 battery cells with 3mm spacing	Parallel air-cooled system	Inlet width = Outlet width = 20mm; Inlet length = Outlet length = 100 mm	Inlet airflow rate = 0.012 m^3/s; Initial air temperature = 300 K	▪ Reducing inlet air temperature can only limit absolute temperature within the battery pack and not the intercellular gradient ▪ Better cooling performance is achieved by placing a secondary vent against the air outlet. Also, increasing width of the secondary vent has a positive effect on cooling performance of the system
Jiaqiang et al. [148]/Computational Modeling		Cold plate having rectangular channels	Aluminium cold plate; Coolant: Water	Discharge Rate = 0.5 to 3C; Coolant velocity = 0.01 to 0.05 m/s; Channel number = 2 – 5; Channel Height = 3 – 6mm	▪ In a cooling plate design, number of channels and coolant flow rate are the primary design factors. ▪ Effect of channel width and height is less in comparison to the primary factors. ▪ For a cold plate with 45mm wide and 5mm high rectangular channels, optimum number of channels is 4 and preferable coolant velocity is 0.07 m/s.
Ling et al. [149]/ Experimental	Twenty 2.6 Ah 18650 Samsung cells in 4P5S combination	PCM/EG	PCM: 60 wt% RT44HC; PCM/EG composite melting point: 42.8 °C, and PCM/fused silica melting point: 41.5 °C	Ambient temperatures of 5 °C and -10 °C; Discharge Rates = 0.5 to 2C	▪ PCM/EG composite resulted in a more uniform temperature distribution within the pack at -10 °C. ▪ Max intercellular voltage difference of 0.02V was noted for case without PCM at -10 °C ▪ PCM/fused silica caused temperature gradient greater than 12 °C within the pack and is not recommended for low temperature applications
Bahirei et al. [150]/Computational Modeling	Six 5 Ah NCA battery cells in parallel	Liquid cooling – Cold plates	Aluminium cold plates; Coolant: Water; Channel height = 6mm; Initial battery SOC = 70%	Laminar flow; FUDC drive cycle; Initial Temp = 293.15 K; Cold plate thickness = 1 – 5mm	▪ Double channel cooling system provides a more uniform thermal distribution and a lower maximum temperature for identical Reynolds number and cold plate thicknesses ▪ Thicker cold plate is preferred but increasing Reynolds number leads to non-uniform temperature gradient

Chen et al. [151]/Computational Modeling	12 x 2 battery cells	Parallel Air-cooling	Length: inlet = outlet = 100mm; Width: inlet = outlet = 20 mm; Adjacent cell spacing = 2mm; Battery heat generation (HG) = 41408 W/m^3	Air flow rate = 0.012 m^3/s; Initial Temp = 300 K;	- Newton method combined with flow resistance method is found suitable for optimization of air-cooling systems - For fixed inlet flow rate and constant HG, optimum width of divergence plenum and convergence plenum are found to be 1.2mm and 20.0mm, respectively - For fixed power consumption of 0.5162 W, optimum inlet flow rate is calculated as 0.011455 m^3/s
Hussain et al. [152]/ Experimental	Six 3.4 Ah Panasonic cells in series	PCM/Graphene coated nickel (GcN) foam	PCM: Paraffin Graphene mass % = 0.5%; Adjacent cell spacing = 5.74mm	Operating temperatures: 25 °C, 30 °C and 33 °C; Discharge currents: 1.7 A and 2.2 A	- GcN improved thermal conductivity of pure paraffin by 23 times. However, latent heat capacity of the GcN saturated paraffin decreased by 30% 17% lower temperature rise was recorded for pack using GcN coated paraffin as TMS compared to the pack using paraffin with nickel foam for 1.7 A discharge
Yan et al. [153]/ Computational modeling	20 Ah LFP cell	PCM-based composite board	Sandwich structure PCM composite board; Board thickness = 10mm; PCM melting temp = 303.15 K; Latent heat = 225 kJ/kg	Ambient temp = 293.15 K; Discharge rates: 1 – 10C	- PCM composite board not only improves thermal distribution within the battery pack but also limits thermal runaway propagation rate - Using PCM with a higher latent heat capacity improves thermal performance of composite board - PCM with latent heat of 1125 kJ/kg and melting temperature in range of 303.15 K and 323.15 K is recommended for use
Ren et al. [154]/Experimental	Samsung SDI 94 Ah cells connected in 5S2P layout	PCM (liquid to gas phase change)	PCM: Sodium alignate hydrogel film with 99% water content; Film thickness = 2mm	Constant current discharge with 250 A and NEDC drive cycle in room temperature	- Presence of hydrogel film caused a reduction of 40.5% in the rate of pack temperature rise during constant current operation of the pack - During NEDC test, temperature of the pack with hydrogel fil increased by only 0.77 °C against 4.75 °C for the pack operating without this film
Qian et al. [155]/ Computational modeling	5 rectangular cells	Mini-channel cold plate	Cold plates: Aluminium; Coolant: Water; Inlet placed near battery electrodes	Laminar flow; Inlet water temperature = Ambient = 25 °C; Discharge rate = 5C;	- No apparent advantage is derived by using a cold plate with more than 5 channels - Increasing inlet flow rate is a more effective means for reducing temperature difference and maximum temperature in the pack than changing flow direction or channel width

Zhao et al. [156]/ Experimental	Aluminium cylinders with heating rods	PCM + HP	PCM: Paraffin/EG; EG wt fraction = 16%; Sintered – copper HP, diameter 6mm;	Ambient = 20 ± 0.5 °C; Start-up temp = 30 °C; Discharge rate = 5C	- HP can prolong the melting duration for PCM under dynamic situations - Maximum recorded temperature for battery pack is reduced by 33.6% due to PCM addition to the module. Further reduction of 28.9% is achieved after embedding HP in PCM matrix
Al-Zareer et al. [157]/ Computational Modeling	LMO 18650 cylindrical battery cells	PCM (liquid to gas phase change)	PCM: Propane; Pressure of liquid propane = 8.5bar; Saturation temperature = 293.15 K;	Submergence level: 5 - 30% of battery height; Charge/ discharge rate = 7.5C; Test Duration = 600s; Initial SOC = 10%	- Submerging only 5% of battery in liquid propane maintains battery temperature below 39 °C for whole test duration. Increasing the submergence level to 30% brings down the battery temperature to 34 °C - Increasing propane pressure to 10 bar reduces temperature difference in the pack at the cost of maximum temperature, which is increased. This effect is more dominant at low submergence levels
Smith et al. [158]/ Experimental	25 Ah prismatic cell	Liquid cooling – Cold plates	Coolant: 50/50 Water-glycol mixture; Cold plate thickness: 5mm or smaller; Plate material: Aluminium	Ambient temps: 0 °C, 20 °C and 40 °C; Discharge rates: 1 – 6C; Test range: SOC 100% to SOC 20%;	- Coolant channel footprint has a greater influence on thermal performance of a cold plate than flow pattern - Flow patterns, both I- and U-type, create similar degrees of thermal gradient over individual cells - Increasing channel width reduces pressure drop in the plate without affecting average pack temperature
Situ et al. [159]/ Experimental	12 Ah LFP prismatic cell	Quaternary PCM + Air-cooling	PCM: Paraffin + EG + low-density polyethylene + copper mesh; mesh thickness = 0.5mm	Ambient temperature: 25 °C; Discharge rates: 1C and 5C	- Thermal conductivity of Paraffin and EG composite increases by 36.0% after addition of copper mesh to it - Maximum temperature recorded in battery pack with quaternary PCM was found 19.5 °C lower than that in the pack cooled via natural air convection - At 5C discharge, air velocity of 6 m/s maximises heat dissipation from quaternary PCM plate
Wu et al. [160]/ Computational Modeling	12 Ah prismatic cells	PCM	PCM: Paraffin + EG + PGS; Cell spacing = PGS thickness = 1.5mm; PGS thermal conductivity = 800 W/m.K	Initial temperature = Ambient = 298.15 K; Discharge Rate = 5C	- EG mass faction between 15 – 20% is recommended - Performance of PCM/PGS modules with heat transfer coefficients of 50 W/$m^2.K$ is found comparable to normal PCM modules of HT coefficients 200 W/$m^2.K$ - Intercellular spacing of 2mm is found sufficient to mitigate thermal runaway propagation in PCM/PGS module. In contrast, 14mm gap between adjacent cells is required in modules filled with normal PCM

Mortazavi et al. [161]/Computational Modeling	6 Ah LCO cell based on 4.4 Ah Hitachi battery	PCM	Paraffin reinforced with graphene nano-membranes; Nanofillers' thickness = 10 nm; Volume concentration: 1% and 4%	Discharge Rates: 0.2C, 1C and 3C; Initial SOC = 98%	- Hexagonal Boron Nitride (hBN) flakes are recommended over graphene nanofillers for addition to paraffin module owing to their superior heat capacity and electrically insulating nature - Graphite network embedded in paraffin provides better thermal performance than TMS designed using graphene nanoparticles
Putra et al. [162]/Experimental	Aluminium alloy battery simulator	Flat plate loop HP	Evaporator: Copper; Capillary wick: stainless steel screen of mesh size 300; Coolant filling ratio: 60%;	Coolants: Distilled water, 96% Alcohol, 95% Acetone; Thermostatic bath temperature: 28 °C	- For heat flux of 1.61 W/m^2, both acetone and alcohol maintained evaporator temperature below 50 °C. In case of distilled water, temperature rises to 60 °C - Acetone results in minimum temperature difference, between the evaporator and the condenser, among the three working fluids throughout the experiment
Hussain et al. [163]/Experimental	Six 3.4 Ah Li-ion cells in series	PCM with nickel foam	Paraffin (Rubitherm 42); Melting range: 38-41 °C; Intercellular spacing = 5.74 mm	Ambient temp: 25 °C; Discharge Rates: 0.5C, 1C and 2C	- Nickel-paraffin composite reduces battery surface temperature by 24% in comparison to pure paraffin during 2C discharge - Decreasing metal foam porosity enhances heat transfer rate thus reducing battery temperature - Discharge capacity increases with increasing porosity
Xie et al. [164]/Computation Modeling	10 Li-ion battery cells	Forced air cooling	Height: air inlet = air outlet = 20mm; Intercellular spacing: 6mm	Ambient temp: 25 °C; Discharge current: 20A; Air flow velocity: 3 m/s	- The temperature difference and the maximum temperature are reduced by 29.72% and 12.82%, respectively, using multi-objective optimization - Evenly spaced channels with inlet angle = outlet angle of 2.5° provides greater temperature uniformity and lowest maximum temperature in the battery pack
Xu et al. [165]/ Computational Modeling	Five 55 Ah prismatic cells	Mini-channel cold plate	Extruded multiport Aluminium channel (h x w x t) = 3 x 3 x 1mm; Coolant: Water	Initial temp = 27 °C; Flow rate = 10 L/min; Nail Diameter: 3 – 5 mm; Nail penetration depth: 20 to 60 mm	- Thermal runaway will be initiated much sooner if a thicker nail penetrates a battery cell or if the nail penetration depth is greater. Also, the maximum temperature reached will be higher in these cases - Mini-channel cooling system with independent control strategy at cellular level can prevent thermal runaway from propagating to adjacent battery cells

Table 2: State-of-the-art battery thermal management systems developed since 2016 (HP: Heat Pipe; EG: Expanded Graphite; PGS: Pyrolytic Graphite Sheets)

4. Emerging Techniques

Several other cooling techniques have been developed in recent times. These techniques offer many advantages, including significant energy and cost-saving potential along with high scalability, over traditional forced-air or liquid cooling methods. In this section, some of these emerging alternatives are discussed in relation to TMS applications.

4.1. Thermoelectric Coolers

Thermoelectric coolers (TECs) are practically maintenance-free solid-state heat pumps with no moving parts. They utilise doped semiconductor elements, comprising of a series of p-type and n-type thermo-elements, sandwiched in thermally-conductive but electrically-insulating substrates to transfer heat across a junction of two dissimilar materials via the Peltier effect. The p-type material has excess positive charge carriers called holes, whereas n-type material carries more negative charge carriers or electrons. The direction of heat transfer depends on the polarity of voltage applied to the TE modules. An illustration of a TEC module is provided in **Fig. 5**.

As voltage is applied to a TEC, electrons jump from a lower energy level of the p-type thermo-element to a higher energy state in the n-type thermo-element by absorbing thermal energy from one side of the module, in effect cooling it. The electrons drop to a stable energy level by rejecting this heat on the other side of the TEC module. Accordingly, the same TEC module can be made to function both as a cooler and as a heater by reversing the direction of current flow across the junction.
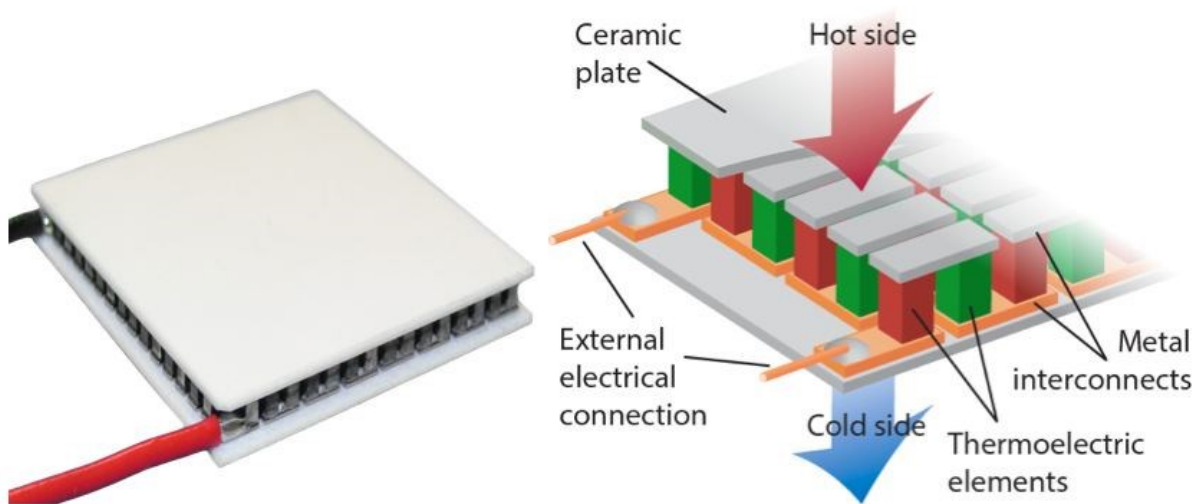
Figure 5: Illustration of a thermo-electric cooling module [166]

Other advantages of TEC are:

- It is compact and lightweight

- It is acoustically silent and operates without any vibrations

- It facilitates precise temperature control to within ±0.1 °C

- It has low manufacturing costs and a wide operating temperature range

- It can cool below ambient temperature

- It is location independent, and can operate in any spatial orientation, at high G-levels or in zero gravity

More importantly, the cooling elements of a TE module are easily scalable [167-169]. For these reasons, TECs have been previously applied for climate control in EVs [170-173]. However, the figure of merit (*ZT*) for the currently available bellerium telluride based TECs is approximately 1. Consequently, the maximum coefficient of performance obtainable with these devices is limited to 10%. It has been suggested that a *ZT* close to 4 is required to achieve cooling performance comparable to other thermal management techniques [174]. Research to develop new thermoelectric material and achieve much higher ZT is, therefore, required to

promote TECs as a viable solution for the temperature control of EV battery packs. Nonetheless, the thermoelectric refrigeration method has been used in the new battery thermal management system developed by the Gentherm Incorporation, details of which are disclosed in US patent 8974942. This patent presents the design of a highly integrated yet simplified assembly of thermoelectric modules that can heat and cool separate battery cells simultaneously [175]. It is, therefore, believed that owing to their flexible form and scalability, TECs may prove pivotal to the development of modular battery packs.

4.2. Thermo-acoustic refrigeration

It is known that thermal gradients can result in sound generation; the interaction between thermodynamics and acoustics can therefore also be utilised to produce a refrigerating effect. Thermo-acoustic refrigerators (TARs) are based on the Stirling cycle and use resonant high intensity sound waves and a compressible mixture of inert gases as working fluid to pump heat. A TAR assembly includes a gas-filled resonance tube containing a regenerative unit, called a stack or regenerator for the respective heat pumping processes, and two heat exchangers. **Fig. 6** shows the cross-sectional layout of a TAR with the different components.

The regenerative unit is a set of concentric cylinders, square rods or uniformly spaced parallel plates strategically arranged between two heat exchangers, such that they reside between the velocity node and antinodes within the resonance tube. Further, an acoustic driver like an electric transducer, a moving-coil loudspeaker or a sinusoidal drive mechanism, is placed on one side of the resonance tube while the other end is closed [176, 177]. The selection of the appropriate driver is based on the design requirements, such as light weight, weight-to-volume ratio, high *BI*-factor and low vibration losses [178].
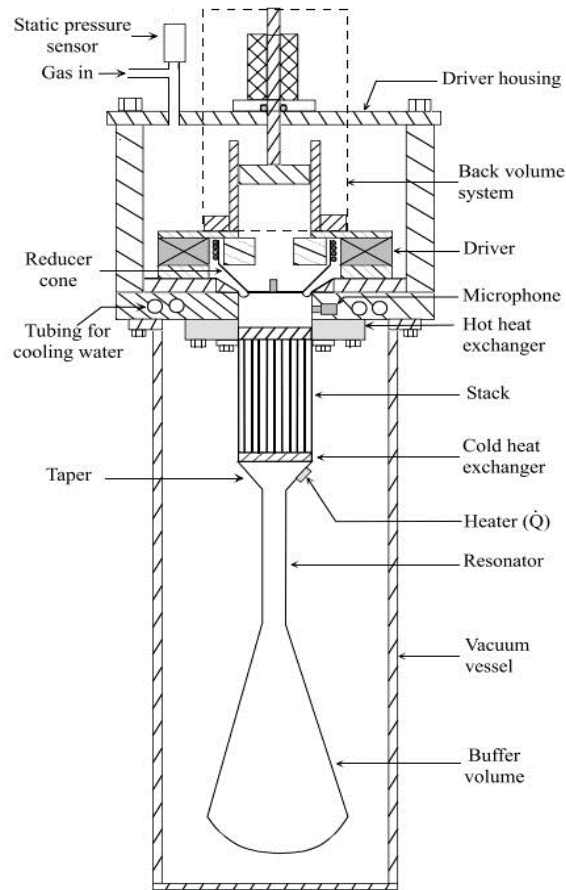
Figure 6: Cross-section of thermoacoustic refrigerator illustrating various parts [178]

The acoustic driver produces cyclic variations of acoustic pressure in the resonance tube, which causes expansion and compression of the inert gases contained in it. In response, the working fluid starts to oscillate in the resonance tube. Imperfect thermal contact of the regenerative unit with the acoustically oscillating gaseous mixture creates necessary phasing. This enables the regenerative unit to continuously absorb heat from the resonance tube at the end near the velocity antinode and reject it to tube walls closer to the velocity node. This natural phasing also allows the TAR to operate without requiring moving parts other than the oscillating working fluid [179, 180]. TARs can achieve heat transfer either via a standing pressure wave or by means of a travelling pressure wave. These two differ in phasing between pressure and velocity. As a result of this phasing, regenerative units with large channels are required in standing pressure wave devices to artificially delay the heat exchange between the tube walls

and the stack. Conversely, much smaller flow channels can be utilised for travelling pressure wave refrigerators, as heat transfer starts immediately after the working fluid is subjected to a pressure change. They are therefore more efficient and compact than standing pressure wave pumps.

Thermoacoustic pumps utilising standing pressure waves perform a surface heat pumping process, whereas travelling pressure waves are used in a conventional Stirling-cycle heat pumping process [181, 182]. TARs require no lubrication, sliding seals or expensive components. They can be manufactured using only low-tolerance machined parts. Furthermore, existing vibrations can be readily isolated in TARs, as they use compressors of low moving mass (approximately 15 gm) and high oscillation frequencies (~ 400 Hz) [179]. The absence of moving parts and vibrations and low manufacturing costs make TARs excellent candidates for battery TMS in EVs.

4.3. Magnetic Refrigeration

Certain ferromagnetic materials and paramagnetic solids are characterised by the intrinsic coupling of their crystal lattice to the external magnetic field. They are called magnetocaloric materials and this coupling is known as the magnetocaloric effect. Under adiabatic conditions, it is quantified by a reversible temperature change observed in the magnetic solid due to variation in its magnetic entropy upon exposure to a varying external magnetic field [183].

The application of a magnetic field induces spin polarisation in magnetocaloric materials, which makes their molecules more stable, thus reducing their degrees of freedom and magnetic entropy. As the total entropy of a magnetic solid remains constant if adiabatic conditions are maintained, vibrations in the crystal lattice and the entropy of free electrons in the material increase to compensate for the lost magnetic entropy. Consequently, an increase in material temperature is noted. In contrast, a cooling effect is observed as the molecular magnetic

ordering returns to the initial alignment state by absorbing thermal energy from the crystal lattice and free electrons when the externally-applied magnetic field is removed [184]. Typically, a field change of 1 Tesla can cause the material temperature to change between 1.5 to 2 K, depending upon the strength of the applied magnetic field and the absolute temperature, but the effect maximises around the Curie or phase transition temperature of the magnetocaloric material [185, 186].
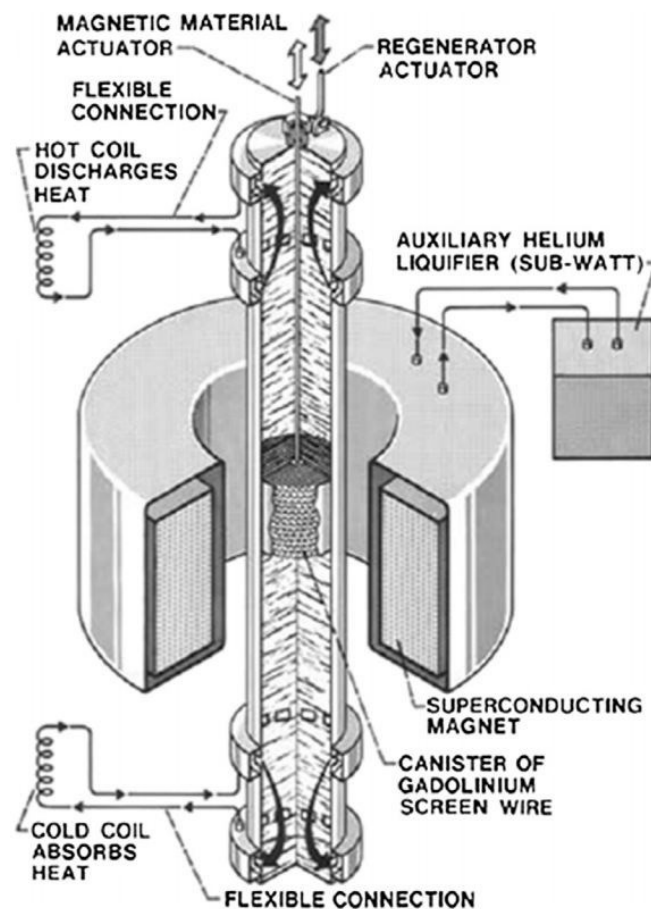
Figure 7: Illustration of an active magnetic regenerator used for room-temperature applications [187].

Magnetic refrigerators for room temperature applications utilise active magnetic regenerators (AMRs) similar to that shown in **Fig. 7**. An AMR combines the functionality of an indirect heat exchanger with a heating/cooling mechanism. It has a porous structure and is made up of magnetocaloric materials like gadolinium and perovskite manganese oxides [188], to maximise the adiabatic temperature span associated with the refrigeration cycle. In this device, the

regenerator is maintained near the Curie temperature and an external magnetic field is periodically applied to it, making it circle in a magnetic entropy-temperature loop. Subsequently, a heat transfer fluid, usually helium or hydrogen gas or a water-based solution, is circulated through the porous structure of the regenerator from the cold end to the hot end. A thermal wave front is established as the working fluid traverses the structure absorbing heat from it. The heat is then discharged to a hot bath at temperatures greater than the bulk temperature. The fluid flow is terminated when the wave front reaches the hot end of the regenerator, i.e. the exiting temperature drops to the hot bath temperature. This also acts as a signal to start the adiabatic demagnetisation of the regenerator followed by the circulation of the working fluid in the reverse direction, completing one refrigeration cycle [189, 190].

Magnetic refrigerators can operate at 30 to 60% efficiency of the Carnot cycle without needing much maintenance [191]. Moreover, they do not need components with large mass rotating or reciprocating at high speeds. They can therefore be compact and virtually noise-free. In addition, they can also provide energy savings of up to 50% in comparison with conventional refrigeration methods [192, 193]. Magnetic refrigeration systems with cooling powers between 200 W and 700 W and a quasi-indefinite lifespan are commercially available for applications such as beverage dispensers, medical refrigerators and wine cellars [194]. It is likely that EV battery packs can also benefit from TMSs based on magnetic refrigeration techniques.

4.4. Internal Cooling

Conventional TMSs minimise thermal gradients across the battery pack by maintaining the exterior cell surface temperature in a pre-specified range. However, a variety of thermal resistances and consequently a large thermal gradient exist in the space separating the heat-generation sites inside the cell from the heat-transfer medium outside it. Estimates for a 26650 Li-ion battery cell suggest that the cell surface temperature and the core temperature may differ by as much as 24 °C for a 10C discharge rate [195]. To address this issue, US patent 6653002

discloses an internal cooling strategy aimed at minimising the thermal resistance between the internal heat-generation sites and the heat-transfer medium.

In one of the embodiments of this invention, microporous TECs are integrated both on the internal and on the external sections of the battery cell. In addition, an array of small heat pipes with a loop or any other open shape is sandwiched between the TECs, forming a cooling module. The open shape of the heat pipes facilitates electrolyte movement in the battery cell. It is also suggested that TECs could be replaced with micro-coolers to accomplish an ultrathin module assembly. If the temperature inside the battery cell becomes greater than the pre-set threshold values established by a temperature controller, electric current is applied to the TEC module and as a result the Peltier effect develops across it. The hot electrolyte flows through the microporous material of the TEC and comes into thermal contact with a cold junction plate, which is essentially a heat sink. The cold plate removes heat from the hot electrolyte until a lower threshold value is attained. The temperature controller immediately stops current flow to the TEC module and a uniform temperature profile is established inside the battery cell [196].

Driven by a similar objective, Bandhauer and Garimella [197] developed a passive system that uses the liquid-to-vapour phase change process to remove heat generated at local internal locations during battery operation. In their concept, an internal evaporator with micro-channels can be incorporated either directly in the thick current collector or embedded in a sheet of inert material compressed between split current collectors. Excess thermal energy is transferred at the appropriate saturation temperature and pressure to a working fluid flowing through chemically inert micro-channels. The working fluid subsequently undergoes liquid-to-vapour phase change and flows under the buoyancy effect to an external condenser, where it is condensed. The gravitational forces transport the condensed fluid back to the evaporator inlet.

The work of these researchers shows that the saturation temperature has a small influence on system performance.

More recently, Mohammadian et al. [198] demonstrated that the internal cooling technique involving electrolyte as a coolant flowing in rectangular micro-channels is more effective in decreasing the bulk temperature of a battery cell than a water-based external cooling system. These researchers also showed that the same pumping power for the internal cooling system could achieve up to five times the uniform temperature distribution in a battery cell. Shah et al. [199] also investigated the effectiveness of annular air passages and heat pipes and plain copper rods inserted along the axis of cells as an internal cooling system. They found that, depending on the inner diameter of the heat pipes, it is possible to reduce the cell core temperature of 26650 Li-ion battery cells by approximately 18 to 20 °C through internal cooling. An appreciable decrease in core temperature can also be achieved by embedding thin copper rods instead of heat pipes in the core of the battery cell. It was noted that internal cooling with heat pipes can delay the onset of thermal runaway events by facilitating rapid heat dissipation from battery cells.

5. Selection of TMS for Modular Battery Pack

Previous research studies have established several techniques as suitable candidates for application in battery thermal management systems. The selection of a specific technique can therefore be made only after evaluating all the available alternatives. The factors that are traditionally considered in the TMS trade-off analysis include energy efficiency, capital costs, ease of operation, maintenance requirements and reliability. A comprehensive assessment of these techniques was last presented by Rao et al [200].

According to their assessment, cold plate and thermoelectric devices are not recommended for use in commercial systems, owing to their high thermal resistance and low coefficient of performance, respectively.

However, Gentherm Incorporation employs thermoelectric devices in their commercial design, whereas cold plates are used in the GM Volt and Tesla Model S battery packs, signifying that both technologies have improved significantly in recent times. A trade-off analysis, updated based on new information, is presented in **Table 3**. In addition to the traditional factors, cooling techniques are also evaluated for scalability, development state and associated technical risks in the present study. More importantly, emerging alternatives, such as magnetic refrigeration and thermoacoustic refrigeration, are included in the comparison.

It is clear that liquid cooling systems are more effective than air-cooled TMS for large battery packs operating at high discharge rates in ambient temperatures higher than room temperature. Research has also shown that required pumping power for a microchannel cold plate system with a 10.0 L/min water flow rate is just 1.3 W. However, pumping power varies with pressure drop, which increases significantly as viscosity of the coolant in increases. For example, TMS using ethylene glycol as coolant sustains nearly six times more pressure drop than the water cooled TMS with same coolant flow rate [165]. The cold plate generally has a flat shape, which makes its application easy in case of battery packs made of pouch cells and prismatic cells. However, the same shape marginalises contact area in case of cylindrical cells, making heat transfer using a cold plate a less effective process. Although the spot welding requirements and potential leak points are much higher in a coolant-jacket design, it ensures optimal thermal contact for cylindrical cells. A coolant jacket system is designed by integrating fluid inlet and outlet with segregation walls or liquid guideways joining a plurality of cell apertures. Cell apertures are hollow cylinders that are made-to-size for a specific battery cell type. Consequentially, they limit scalability of the jacketed system.

| Criteria | Forced Air | Liquid | | | PCM | Thermoelectric | Thermoacoustic | Magnetic |
		Jacket	Cold Plate	Heat Pipe				
Ease of use	High	Low	Moderate	Moderate	High	Moderate	Moderate	Moderate
Integration	Simple	Difficult	Intermediate	Intermediate	Simple	Intermediate	Intermediate	Difficult
Energy efficiency	Low	High	Medium	High	High	Medium	Medium	High
Thermal gradient	High	Low	Moderate	Moderate	Low	Moderate	Moderate	Low
Cooling level	Small	Large	Medium	Large	Large	Medium	Medium	High
Regeneration rate	High	Medium	High	Medium	Low	High	Medium	High
COP @ room temperature	0.4 – 0.7	1.8 – 2.1	1.5 – 1.9	N/A	N/A	0.7 - 1.2	Up to 1.0	1.8
Maintenance	Low	High	Medium	Medium	Low	Medium	Low	Low
First cost	Low	High	High	High	Moderate	High	Low	Medium
Scalability	High	Low	Low	Low	High	Medium	Medium	High
Technical risks	Low	High	Medium	Medium	Low	Medium	High	Medium
Development state	Commercial	Prototype	Commercial	Prototype	Prototype	Commercial	Experimental	Experimental

Table 3: Qualitative analysis of various battery thermal management methods

Battery packs are designed by connecting multiple battery cells in a series-parallel combination. As a result, they can be rescaled simply by modifying the number of battery cells involved in this combination. However, as soon as a liquid thermal management system is integrated within the electrical-mechanical-structural framework of the batteries, the battery pack loses its configurability. For instance, if the number of modules in the current battery pack architecture needs to be increased to meet energy requirements of a certain application, or if the current pack is too big for the envisioned application and it is decided to do away with the pack's excess energy storage capacity, then the pre-existing piping/plumbing and the auxiliary devices would either be over-engineered or under-designed for the new application and will need to be redesigned. It is, therefore, imperative for battery packs to have a modular thermal management system for them to retain their scalability. In other words, mechanical modularity is dependent on thermal modularity of the system, as heat exchange between neighbouring battery modules cannot be fully eliminated. Hence, thermal independence of adjoining battery modules must be ensured so that structural and mechanical design requirements can be satisfied for the battery pack. Inefficiency in heat transfer due to incompatible geometries and marginalised contact area can be removed via PCMs. PCMs will not only enable a greater control over battery cell temperature and but also provide tight packaging by functioning as a suitable cell spacer and filling up the voids between neighbouring cells. However, low thermal conductivity of PCMs needs to be considered while selecting a suitable thermal management system for EV battery packs.

It is evident from the analysis that none of the thermal management techniques alone can meet the operational requirements of a modular TMS. It can therefore be inferred that a modular TMS would involve a combination of these techniques. In other words, a modular TMS needs to be a hybrid system. After careful consideration of all the likely scenarios, it is estimated that

this hybrid system will be developed around PCM. An example of one such hybrid system is demonstrated in Ref. [201].

Lastly, there are several approaches to designing a TMS. The most appropriate approach depends on the desired level of sophistication, the availability of information, and the timeline/budget for a particular project. A systematic approach, proposed by Pesaran [75, 202], can be adopted for the design of a TMS in general.

6. Conclusions

Different thermal issues affecting performance, cycle life and safety of Li-ion battery packs are briefly discussed in this paper, and various thermal management techniques to address these issues are qualitatively reviewed. The purpose of the review is to assess their suitability for a modular battery pack.

Conventional TMSs like fans and cold plates either have low scalability or deliver marginal performance (estimated from combined sets of cooling levels and regeneration rates) under challenging conditions. Other interesting alternatives are available but they have not yet attained full technological maturity. It is, therefore, concluded that a robust modular TMS would be a hybrid system, designed through the union of at least two different TMSs. Considering factors such as technical risks, ease of integration, cost and energy efficiency, it can be inferred that PCMs would form an integral part of the modular TMS assembly. Thermoelectric devices also appear to be a promising candidate for this application, due to their superior state of development and acceptable COP at room temperatures.

Acknowledgement

References

[1] Spotnitz R, Franklin J. Abuse behavior of high-power, lithium-ion cells. Journal of Power Sources. 2003;113:81-100.

[2] Kulkarni A, Kapoor A, Arora S. Battery Packaging and System Design for an Electric Vehicle. SAE International; 2015.

[3] Arora S, Shen W, Kapoor A. Neural network based computational model for estimation of heat generation in LiFePO4 pouch cells of different nominal capacities. Computers & Chemical Engineering. 2017;101:81-94.

[4] Lin C, Xu S, Chang G, Liu J. Experiment and simulation of a LiFePO4 battery pack with a passive thermal management system using composite phase change material and graphite sheets. Journal of Power Sources. 2015;275:742-9.

[5] Zhu C, Li X, Song L, Xiang L. Development of a theoretically based thermal model for lithium ion battery pack. Journal of Power Sources. 2013;223:155-64.

[6] MacNeil DD, Larcher D, Dahn JR. Comparison of the reactivity of various carbon electrode materials with electrolyte at elevated temperature. Journal of the Electrochemical Society. 1999;146:3596-602.

[7] Suh IS, Cho H, Lee M. Feasibility study on thermoelectric device to energy storage system of an electric vehicle. Energy. 2014;76:436-44.

[8] Kim H, Park S-G, Jung B, Hwang J, Kim W. New device architecture of a thermoelectric energy conversion for recovering low-quality heat. Applied Physics A. 2014;114:1201-8.

[9] Arora S, Kapoor A, Shen W. Application of Robust Design Methodology to Battery Packs for Electric Vehicles: Identification of Critical Technical Requirements for Modular Architecture. Batteries. 2018;4:30.

[10] Arora S, Shen W, Kapoor A. Review of mechanical design and strategic placement technique of a robust battery pack for electric vehicles. Renewable and Sustainable Energy Reviews. 2016;60:1319-31.

[11] Arora S. Design of a modular battery pack for electric vehicles [Doctoral]. Australia: Swinburne University of Technology, Melbourne; 2017.

[12] Bandhauer TM, Garimella S, Fuller TF. A critical review of thermal issues in lithium-ion batteries. Journal of the Electrochemical Society. 2011;158:R1-R25.

[13] Basu S, Hariharan KS, Kolake SM, Song T, Sohn DK, Yeo T. Coupled electrochemical thermal modelling of a novel Li-ion battery pack thermal management system. Applied Energy. 2016;181:1-13.

[14] Nagasubramanian G. Electrical characteristics of 18650 Li-ion cells at low temperatures. Journal of applied electrochemistry. 2001;31:99-104.

[15] Zhang S, Xu K, Jow T. The low temperature performance of Li-ion batteries. Journal of Power Sources. 2003;115:137-40.

[16] Ehrlich GM. Handbook of batteries. McGraw-Hill, NY and London. 2002.

[17] Smart MC, Ratnakumar BV, Surampudi S. Electrolytes for Low-Temperature Lithium Batteries Based on Ternary Mixtures of Aliphatic Carbonates. Journal of the Electrochemical Society. 1999;146:486-92.

[18] Ratnakumar BV, Smart MC, Surampudi S. Effects of SEI on the kinetics of lithium intercalation. J Power Sources. 2001;97-98:137-9.

[19] Lin HP, Chua D, Salomon M, Shiao HC, Hendrickson M, Plichta E, et al. Low-temperature behavior of Li-ion cells. Electrochemical and Solid-State Letters. 2001;4:A71-A3.

[20] Zhang SS, Xu K, Jow TR. Low-temperature performance of Li-ion cells with a LiBF4-based electrolyte. J Solid State Electrochem. 2003;7:147-51.

[21] Wang C, Appleby AJ, Little FE. Low-temperature characterization of lithium-ion carbon Anodes via microperturbation measurement. Journal of the Electrochemical Society. 2002;149:A754-A60.

[22] Arora S, Kapoor A. Mechanical Design and Packaging of Battery Packs for Electric Vehicles. In: Pistoia G, Liaw B, editors. Behaviour of Lithium-Ion Batteries in Electric Vehicles: Battery Health, Performance, Safety, and Cost. Cham: Springer International Publishing; 2018. p. 175-200.

[23] Arora S, Shen W, Kapoor A. Designing a Robust Battery Pack for Electric Vehicles Using a Modified Parameter Diagram. SAE International; 2015.

[24] Blomgren GE. Electrolytes for advanced batteries. Journal of Power Sources. 1999;81-82:112-8.

[25] Joho F, Rykart B, Imhof R, Novák P, Spahr ME, Monnier A. Key factors for the cycling stability of graphite intercalation electrodes for lithium-ion batteries. Journal of Power Sources. 1999;81-82:243-7.

[26] Abe K, Yoshitake H, Kitakura T, Hattori T, Wang H, Yoshio M. Additives-containing functional electrolytes for suppressing electrolyte decomposition in lithium-ion batteries. Electrochimica Acta. 2004;49:4613-22.

[27] Amatucci G, Du Pasquier A, Blyr A, Zheng T, Tarascon J-M. The elevated temperature performance of the LiMn 2 O 4/C system: failure and solutions. Electrochimica Acta. 1999;45:255-71.

[28] Vetter J, Novák P, Wagner MR, Veit C, Möller KC, Besenhard JO, et al. Ageing mechanisms in lithium-ion batteries. Journal of Power Sources. 2005;147:269-81.

[29] Petibon R, Harlow J, Le DB, Dahn JR. The use of ethyl acetate and methyl propanoate in combination with vinylene carbonate as ethylene carbonate-free solvent blends for electrolytes in Li-ion batteries. Electrochimica Acta. 2015;154:227-34.

[30] Smart MC, Ratnakumar BV, Chin KB, Whitcanack LD. Lithium-ion electrolytes containing ester cosolvents for improved low temperature performance. Journal of the Electrochemical Society. 2010;157:A1361-A74.

[31] Zhou L, Xu M, Lucht BL. Performance of lithium tetrafluorooxalatophosphate in methyl butyrate electrolytes. Journal of Applied Electrochemistry. 2013;43:497-505.

[32] Herreyre S, Huchet O, Barusseau S, Perton F, Bodet JM, Biensan P. New Li-ion electrolytes for low temperature applications. J Power Sources. 2001;97-98:576-80.

[33] Plichta EJ, Behl WK. Low-temperature electrolyte for lithium and lithium-ion batteries. Journal of Power Sources. 2000;88:192-6.

[34] Ji Y, Zhang Y, Wang CY. Li-ion cell operation at low temperatures. Journal of the Electrochemical Society. 2013;160:A636-A49.

[35] Yang B, Zhang H, Yu L, Fan W, Huang D. Lithium difluorophosphate as an additive to improve the low temperature performance of LiNi0.5Co0.2Mn0.3O2/graphite cells. Electrochimica Acta. 2016;221:107-14.

[36] Smart MC, Lucht BL, Dalavi S, Krause FC, Ratnakumar BV. The Effect of Additives upon the Performance of MCMB/LiNixCo1– xO2 Li-Ion Cells Containing Methyl Butyrate-Based Wide Operating Temperature Range Electrolytes. Journal of The Electrochemical Society. 2012;159:A739-A51.

[37] Niedzicki L, Grugeon S, Laruelle S, Judeinstein P, Bukowska M, Prejzner J, et al. New covalent salts of the 4+ V class for Li batteries. Journal of Power Sources. 2011;196:8696-700.

[38] Xu K, Zhang S, Jow TR. LiBOB as additive in LiPF6-based lithium ion electrolytes. Electrochemical and Solid-State Letters. 2005;8:A365-A8.

[39] Lazar ML, Lucht BL. Carbonate free electrolyte for lithium ion batteries containing γ-butyrolactone and methyl butyrate. Journal of the Electrochemical Society. 2015;162:A928-A34.

[40] Li S, Zhao W, Zhou Z, Cui X, Shang Z, Liu H, et al. Studies on electrochemical performances of novel electrolytes for wide-temperature-range lithium-ion batteries. ACS Appl Mater Interfaces. 2014;6:4920-6.

[41] Brodd RJ. Batteries for sustainability: selected entries from the encyclopedia of sustainability science and technology: Springer Science & Business Media; 2012.

[42] Groot J. State-of-health estimation of li-ion batteries: Cycle life test methods. 2012.

[43] Kong F, Kostecki R, Nadeau G, Song X, Zaghib K, Kinoshita K, et al. In situ studies of SEI formation. Journal of power sources. 2001;97:58-66.

[44] Richard MN, Dahn JR. Accelerating rate calorimetry study on the thermal stability of lithium intercalated graphite in electrolyte. I. Experimental. Journal of the Electrochemical Society. 1999;146:2068-77.

[45] Yang H, Amiruddin S, Bang H, Sun Y, Prakash J. A review of Li-Ion cell chemistries and their potential use in hybrid electric vehicles. J Ind Eng Chem2006. p. 12-38.

[46] Abraham DP, Roth EP, Kostecki R, McCarthy K, MacLaren S, Doughty DH. Diagnostic examination of thermally abused high-power lithium-ion cells. Journal of Power Sources. 2006;161:648-57.

[47] Al Hallaj S, Maleki H, Hong JS, Selman JR. Thermal modeling and design considerations of lithium-ion batteries. Journal of Power Sources. 1999;83:1-8.

[48] Lisbona D, Snee T. A review of hazards associated with primary lithium and lithium-ion batteries. Process Safety and Environmental Protection. 2011;89:434-42.

[49] Yang H, Amiruddin S, Bang HJ, Sun Y-K, Prakash J. A review of Li-ion cell chemistries and their potential use in hybrid electric vehicles. Journal of industrial and engineering chemistry. 2006;12:12-38.

[50] Ross PE. Boeing's Battery Blues. 2013.

[51] Etacheri V, Marom R, Elazari R, Salitra G, Aurbach D. Challenges in the development of advanced Li-ion batteries: a review. Energy & Environmental Science. 2011;4:3243-62.

[52] MacNeil DD, Lu Z, Chen Z, Dahn JR. A comparison of the electrode/electrolyte reaction at elevated temperatures for various Li-ion battery cathodes. Journal of Power Sources. 2002;108:8-14.

[53] Zhang J, Gao R, Sun L, Zhang H, Hu Z, Liu X. Unraveling the multiple effects of Li2ZrO3 coating on the structural and electrochemical performances of LiCoO2 as high-voltage cathode materials. Electrochimica Acta. 2016;209:102-10.

[54] Ji Y, Wang CY. Heating strategies for Li-ion batteries operated from subzero temperatures. Electrochimica Acta. 2013;107:664-74.

[55] Zhang S, Xu K, Jow T. Charge and discharge characteristics of a commercial LiCoO 2-based 18650 Li-ion battery. Journal of Power Sources. 2006;160:1403-9.

[56] Nakayama Y, Mitsui M, Kikuchi Y, Tojima K. Apparatus for controlling state of charge/discharge of hybrid car and method for controlling state of charge/discharge of hybrid car. Google Patents; 2000.

[57] Zhu D, Mathews J, Taenaka B, Maguire P. Method and system for a vehicle battery temperature control. Google Patents; 2006.

[58] Horie H, Ohsawa Y. Battery system with excellent controllability for temperature. Google Patents; 2007.

[59] Pesaran A, Vlahinos A, Stuart T. Cooling and preheating of batteries in hybrid electric vehicles. 6th ASME-JSME Thermal Engineering Joint Conference: Citeseer; 2003. p. 1-7.

[60] Vlahinos A, Pesaran AA. Energy efficient battery heating in cold climates. SAE Technical Paper; 2002.

[61] Stuart T, Hande A. HEV battery heating using AC currents. Journal of Power Sources. 2004;129:368-78.

[62] Mahamud R, Park C. Reciprocating air flow for Li-ion battery thermal management to improve temperature uniformity. Journal of Power Sources. 2011;196:5685-96.

[63] Li X, He F, Ma L. Thermal management of cylindrical batteries investigated using wind tunnel testing and computational fluid dynamics simulation. Journal of Power Sources. 2013;238:395-402.

[64] Xu XM, He R. Research on the heat dissipation performance of battery pack based on forced air cooling. Journal of Power Sources. 2013;240:33-41.

[65] Fan L, Khodadadi JM, Pesaran AA. A parametric study on thermal management of an air-cooled lithium-ion battery module for plug-in hybrid electric vehicles. Journal of Power Sources. 2013;238:301-12.

[66] Park H. A design of air flow configuration for cooling lithium ion battery in hybrid electric vehicles. Journal of Power Sources. 2013;239:30-6.

[67] Giuliano MR, Prasad AK, Advani SG. Experimental study of an air-cooled thermal management system for high capacity lithium-titanate batteries. Journal of Power Sources. 2012;216:345-52.

[68] Lou Y. Nickel-metal hydride battery cooling system research for hybrid electric vehicle. Shanghai Jiao Tong University, Shanghai. 2007.

[69] Jaura AK, Park C-W. Battery system for automotive vehicle. Google Patents; 2007.

[70] He F, Ma L. Thermal management of batteries employing active temperature control and reciprocating cooling flow. International Journal of Heat and Mass Transfer. 2015;83:164-72.

[71] He F, Wang H, Ma L. Experimental demonstration of active thermal control of a battery module consisting of multiple Li-ion cells. International Journal of Heat and Mass Transfer. 2015;91:630-9.

[72] Wu MS, Liu KH, Wang YY, Wan CC. Heat dissipation design for lithium-ion batteries. Journal of Power Sources. 2002;109:160-6.

[73] Nelson P, Dees D, Amine K, Henriksen G. Modeling thermal management of lithium-ion PNGV batteries. Journal of Power Sources. 2002;110:349-56.

[74] Pendergast DR, Demauro EP, Fletcher M, Stimson E, Mollendorf JC. A rechargeable lithium-ion battery module for underwater use. Journal of Power Sources. 2011;196:793-800.

[75] Pesaran AA. Battery thermal management in EV and HEVs: issues and solutions. Battery Man. 2001;43:34-49.

[76] Pesaran AA, Burch S, Keyser M. An approach for designing thermal management systems for electric and hybrid vehicle battery packs. Proceedings of the 4th Vehicle Thermal Management Systems. 1999;24-7.

[77] Xia G, Cao L, Bi G. A review on battery thermal management in electric vehicle application. Journal of Power Sources. 2017;367:90-105.

[78] Kim G, Pesaran A. 22nd International Battery. Hybrid and Fuel Cell Electric Vehicle Conference and Exhibition, Yokohama, Japan2006.

[79] Jarrett A, Kim IY. Design optimization of electric vehicle battery cooling plates for thermal performance. Journal of Power Sources. 2011;196:10359-68.

[80] Fisher TS, Torrance KE. Optimal shapes of fully embedded channels for conjugate cooling. IEEE Trans Adv Packag. 2001;24:555-62.

[81] Fisher T, Torrance K. Constrained optimal duct shapes for conjugate laminar forced convection. International journal of heat and mass transfer. 2000;43:113-26.

[82] Yu SH, Sohn S, Nam JH, Kim CJ. Numerical study to examine the performance of multi-pass serpentine flow-fields for cooling plates in polymer electrolyte membrane fuel cells. Journal of Power Sources. 2009;194:697-703.

[83] Choi J, Kim YH, Lee Y, Lee KJ, Kim Y. Numerical analysis on the performance of cooling plates in a PEFC. J Mech Sci Technol. 2008;22:1417-25.

[84] Chen FC, Gao Z, Loutfy RO, Hecht M. Analysis of Optimal Heat Transfer in a PEM Fuel Cell Cooling Plate. Fuel Cells. 2003;3:181-8.

[85] Jin LW, Lee PS, Kong XX, Fan Y, Chou SK. Ultra-thin minichannel LCP for EV battery thermal management. Applied Energy. 2014;113:1786-94.

[86] Huo Y, Rao Z, Liu X, Zhao J. Investigation of power battery thermal management by using mini-channel cold plate. Energy Conversion and Management. 2015;89:387-95.

[87] Saw LH, Poon HM, Thiam HS, Cai Z, Chong WT, Pambudi NA, et al. Novel thermal management system using mist cooling for lithium-ion battery packs. Applied Energy. 2018;223:146-58.

[88] Al-Zareer M, Dincer I, Rosen MA. Development and evaluation of a new ammonia boiling based battery thermal management system. Electrochimica Acta. 2018;280:340-52.

[89] Lytron. The Best Heat Transfer Fluids for Liquid Cooling. Application Notes2018.

[90] Pipe.nl H. Dutch knowledge center for heat pipe technology - The basics. 2010.

[91] Mahefkey E, Kreitman M. An Intercell Planar Heat Pipe for the Removal of Heat During the Cycling of a High Rate Nickel Cadmium Battery. Journal of The Electrochemical Society. 1971;118:1382-6.

[92] ZHANG G, WU Z, RAO Z, FU L. Experimental invesitigation on heat pipe cooling effect for power battery [J]. Chemical Industry and Engineering Progress. 2009;7:013.

[93] Swanepoel G. Thermal management of hybrid electrical vehicles using heat pipes: University of Stellenbosch; 2001.

[94] Wu M-S, Liu K, Wang Y-Y, Wan C-C. Heat dissipation design for lithium-ion batteries. Journal of power sources. 2002;109:160-6.

[95] Jang J-C, Rhi S-H. Battery thermal management system of future electric vehicles with loop thermosyphon. US-Korea conference on science, technology, and entrepreneurship (UKC)2010.

[96] Rao Z, Wang S, Wu M, Lin Z, Li F. Experimental investigation on thermal management of electric vehicle battery with heat pipe. Energy Conversion and Management. 2013;65:92-7.

[97] Connors MJ, Zunner JA. The use of vapor chambers and heat pipes for cooling military embedded electronic devices. Military Communications Conference, 2009 MILCOM 2009 IEEE: IEEE; 2009. p. 1-7.

[98] Guo C, Hu X, Cao W, Yu D, Tang D. Effect of mechanical vibration on flow and heat transfer characteristics in rectangular microgrooves. Applied Thermal Engineering. 2013;52:385-93.

[99] Thompson SM, Aspin ZS, Shamsaei N, Elwany A, Bian L. Additive manufacturing of heat exchangers: A case study on a multi-layered Ti–6Al–4V oscillating heat pipe. Additive Manufacturing. 2015;8:163-74.

[100] Ameli M, Agnew B, Leung PS, Ng B, Sutcliffe C, Singh J, et al. A novel method for manufacturing sintered aluminium heat pipes (SAHP). Applied Thermal Engineering. 2013;52:498-504.

[101] Chen Y-T, Kang S-W, Hung Y-H, Huang C-H, Chien K-C. Feasibility study of an aluminum vapor chamber with radial grooved and sintered powders wick structures. Applied Thermal Engineering. 2013;51:864-70.

[102] Ibrahim OT, Monroe JG, Thompson SM, Shamsaei N, Bilheux H, Elwany A, et al. An investigation of a multi-layered oscillating heat pipe additively manufactured from Ti-6Al-4V powder. International Journal of Heat and Mass Transfer. 2017;108:1036-47.

[103] GeneralElectricCompany. Advantages of Closed Systems - Scale Control. Closed Recirculating Cooling Systems2012.

[104] Liu X, Zhang X, Lu T, Mahkamov K, Wu H, Mirzaeian M. Numerical simulation of sub-cooled boiling flow with fouling deposited inside channels. Applied Thermal Engineering. 2016;103:434-42.

[105] SchneiderElectric. Why choose glycol over water? APC - Life is On2018.

[106] Selvam C, Lal DM, Harish S. Thermal conductivity enhancement of ethylene glycol and water with graphene nanoplatelets. Thermochimica Acta. 2016;642:32-8.

[107] Sarafraz MM, Nikkhah V, Nakhjavani M, Arya A. Fouling formation and thermal performance of aqueous carbon nanotube nanofluid in a heat sink with rectangular parallel microchannel. Applied Thermal Engineering. 2017;123:29-39.

[108] Kuruneru STW, Sauret E, Saha SC, Gu Y. Coupled CFD-DEM simulation of oscillatory particle-laden fluid flow through a porous metal foam heat exchanger: Mitigation of particulate fouling. Chemical Engineering Science. 2018;179:32-52.

[109] Tijing LD, Kim HY, Lee DH, Kim CS, Cho YI. Use of an Oscillating Electric Field to Mitigate Mineral Fouling in a Heat Exchanger. Experimental Heat Transfer. 2009;22:257-70.

[110] Al Hallaj S, Selman J. A Novel Thermal Management System for Electric Vehicle Batteries Using Phase-Change Material. Journal of the Electrochemical Society. 2000;147:3231-6.

[111] Hallaj SA, Selman JR. Thermal management of battery systems. Google Patents; 2002.

[112] Jaguemont J, Omar N, Van den Bossche P, Mierlo J. Phase-change materials (PCM) for automotive applications: A review. Applied Thermal Engineering. 2018;132:308-20.

[113] Khateeb SA, Farid MM, Selman JR, Al-Hallaj S. Design and simulation of a lithium-ion battery with a phase change material thermal management system for an electric scooter. Journal of Power Sources. 2004;128:292-307.

[114] Mills A, Al-Hallaj S. Simulation of passive thermal management system for lithium-ion battery packs. Journal of Power Sources. 2005;141:307-15.

[115] Sabbah R, Kizilel R, Selman JR, Al-Hallaj S. Active (air-cooled) vs. passive (phase change material) thermal management of high power lithium-ion packs: Limitation of temperature rise and uniformity of temperature distribution. Journal of Power Sources. 2008;182:630-8.

[116] Kizilel R, Lateef A, Sabbah R, Farid MM, Selman JR, Al-Hallaj S. Passive control of temperature excursion and uniformity in high-energy Li-ion battery packs at high current and ambient temperature. Journal of Power Sources. 2008;183:370-5.

[117] Rao Z, Wang S, Zhang G. Simulation and experiment of thermal energy management with phase change material for ageing LiFePO4 power battery. Energy Conversion and Management. 2011;52:3408-14.

[118] Li W, Qu Z, He Y, Tao Y. Experimental study of a passive thermal management system for high-powered lithium ion batteries using porous metal foam saturated with phase change materials. Journal of power sources. 2014;255:9-15.

[119] Arora S, Shen W, Kapoor A. Critical analysis of open circuit voltage and its effect on estimation of irreversible heat for Li-ion pouch cells. Journal of Power Sources. 2017;350:117-26.

[120] Alrashdan A, Mayyas AT, Al-Hallaj S. Thermo-mechanical behaviors of the expanded graphite-phase change material matrix used for thermal management of Li-ion battery packs. Journal of Materials Processing Technology. 2010;210:174-9.

[121] Fan L, Khodadadi JM. Thermal conductivity enhancement of phase change materials for thermal energy storage: a review. Renewable and Sustainable Energy Reviews. 2011;15:24-46.

[122] Shatikian V, Ziskind G, Letan R. Numerical investigation of a PCM-based heat sink with internal fins: constant heat flux. International Journal of Heat and Mass Transfer. 2008;51:1488-93.

[123] Agyenim F, Eames P, Smyth M. A comparison of heat transfer enhancement in a medium temperature thermal energy storage heat exchanger using fins. Solar Energy. 2009;83:1509-20.

[124] Nakaso K, Teshima H, Yoshimura A, Nogami S, Hamada Y, Fukai J. Extension of heat transfer area using carbon fiber cloths in latent heat thermal energy storage tanks. Chemical Engineering and Processing: Process Intensification. 2008;47:879-85.

[125] Ettouney H, Alatiqi I, Al-Sahali M, Al-Hajirie K. Heat transfer enhancement in energy storage in spherical capsules filled with paraffin wax and metal beads. Energy Conversion and Management. 2006;47:211-28.

[126] Ling Z, Chen J, Fang X, Zhang Z, Xu T, Gao X, et al. Experimental and numerical investigation of the application of phase change materials in a simulative power batteries thermal management system. Applied Energy. 2014;121:104-13.

[127] Mills A, Farid M, Selman J, Al-Hallaj S. Thermal conductivity enhancement of phase change materials using a graphite matrix. Applied Thermal Engineering. 2006;26:1652-61.

[128] Zhang Z, Fang X. Study on paraffin/expanded graphite composite phase change thermal energy storage material. Energy Conversion and Management. 2006;47:303-10.

[129] Li W, Qu Z, He Y, Tao W. Experimental and numerical studies on melting phase change heat transfer in open-cell metallic foams filled with paraffin. Applied Thermal Engineering. 2012;37:1-9.

[130] Zhao C-Y, Lu W, Tian Y. Heat transfer enhancement for thermal energy storage using metal foams embedded within phase change materials (PCMs). Solar Energy. 2010;84:1402-12.

[131] Lafdi K, Mesalhy O, Shaikh S. Experimental study on the influence of foam porosity and pore size on the melting of phase change materials. Journal of Applied Physics. 2007;102:083549.

[132] Zhou D, Zhao CY. Experimental investigations on heat transfer in phase change materials (PCMs) embedded in porous materials. Applied Thermal Engineering. 2011;31:970-7.

[133] Xiao X, Zhang P, Li M. Preparation and thermal characterization of paraffin/metal foam composite phase change material. Applied energy. 2013;112:1357-66.

[134] Wang H, Wang F, Li Z, Tang Y, Yu B, Yuan W. Experimental investigation on the thermal performance of a heat sink filled with porous metal fiber sintered felt/paraffin composite phase change material. Applied Energy. 2016;176:221-32.

[135] Chen P, Gao X, Wang Y, Xu T, Fang Y, Zhang Z. Metal foam embedded in SEBS/paraffin/HDPE form-stable PCMs for thermal energy storage. Solar Energy Materials and Solar Cells. 2016;149:60-5.

[136] Hussain A, Tso CY, Chao CY. Experimental investigation of a passive thermal management system for high-powered lithium ion batteries using nickel foam-paraffin composite. Energy. 2016;115:209-18.

[137] Goli P, Legedza S, Dhar A, Salgado R, Renteria J, Balandin AA. Graphene-enhanced hybrid phase change materials for thermal management of Li-ion batteries. Journal of Power Sources. 2014;248:37-43.

[138] Babapoor A, Azizi M, Karimi G. Thermal management of a Li-ion battery using carbon fiber-PCM composites. Applied Thermal Engineering. 2015;82:281-90.

[139] Frusteri F, Leonardi V, Vasta S, Restuccia G. Thermal conductivity measurement of a PCM based storage system containing carbon fibers. Applied Thermal Engineering. 2005;25:1623-33.

[140] Wang W, Yang X, Fang Y, Ding J, Yan J. Enhanced thermal conductivity and thermal performance of form-stable composite phase change materials by using β-Aluminum nitride. Applied Energy. 2009;86:1196-200.

[141] Khateeb SA, Amiruddin S, Farid M, Selman JR, Al-Hallaj S. Thermal management of Li-ion battery with phase change material for electric scooters: experimental validation. Journal of Power Sources. 2005;142:345-53.

[142] Huang Q, Li X, Zhang G, Zhang J, He F, Li Y. Experimental investigation of the thermal performance of heat pipe assisted phase change material for battery thermal management system. Applied Thermal Engineering. 2018;141:1092-100.

[143] Liang J, Gan Y, Li Y. Investigation on the thermal performance of a battery thermal management system using heat pipe under different ambient temperatures. Energy Conversion and Management. 2018;155:1-9.

[144] Wu W, Yang X, Zhang G, Chen K, Wang S. Experimental investigation on the thermal performance of heat pipe-assisted phase change material based battery thermal management system. Energy Conversion and Management. 2017;138:486-92.

[145] Ye X, Zhao Y, Quan Z. Experimental study on heat dissipation for lithium-ion battery based on micro heat pipe array (MHPA). Applied Thermal Engineering. 2018;130:74-82.

[146] Wang Q, Rao Z, Huo Y, Wang S. Thermal performance of phase change material/oscillating heat pipe-based battery thermal management system. International Journal of Thermal Sciences. 2016;102:9-16.

[147] Hong S, Zhang X, Chen K, Wang S. Design of flow configuration for parallel air-cooled battery thermal management system with secondary vent. International Journal of Heat and Mass Transfer. 2018;116:1204-12.

[148] E J, Han D, Qiu A, Zhu H, Deng Y, Chen J, et al. Orthogonal experimental design of liquid-cooling structure on the cooling effect of a liquid-cooled battery thermal management system. Applied Thermal Engineering. 2018;132:508-20.

[149] Ling Z, Wen X, Zhang Z, Fang X, Gao X. Thermal management performance of phase change materials with different thermal conductivities for Li-ion battery packs operated at low temperatures. Energy. 2018;144:977-83.

[150] Bahiraei F, Fartaj A, Nazri G-A. Electrochemical-thermal Modeling to Evaluate Active Thermal Management of a Lithium-ion Battery Module. Electrochimica Acta. 2017;254:59-71.

[151] Chen K, Wang S, Song M, Chen L. Structure optimization of parallel air-cooled battery thermal management system. International Journal of Heat and Mass Transfer. 2017;111:943-52.

[152] Hussain A, Abidi IH, Tso CY, Chan KC, Luo Z, Chao CYH. Thermal management of lithium ion batteries using graphene coated nickel foam saturated with phase change materials. International Journal of Thermal Sciences. 2018;124:23-35.

[153] Yan J, Wang Q, Li K, Sun J. Numerical study on the thermal performance of a composite board in battery thermal management system. Applied Thermal Engineering. 2016;106:131-40.

[154] Ren Y, Yu Z, Song G. Thermal management of a Li-ion battery pack employing water evaporation. Journal of Power Sources. 2017;360:166-71.

[155] Qian Z, Li Y, Rao Z. Thermal performance of lithium-ion battery thermal management system by using mini-channel cooling. Energy Conversion and Management. 2016;126:622-31.

[156] Zhao J, Lv P, Rao Z. Experimental study on the thermal management performance of phase change material coupled with heat pipe for cylindrical power battery pack. Experimental Thermal and Fluid Science. 2017;82:182-8.

[157] Al-Zareer M, Dincer I, Rosen MA. Novel thermal management system using boiling cooling for high-powered lithium-ion battery packs for hybrid electric vehicles. Journal of Power Sources. 2017;363:291-303.

[158] Smith J, Hinterberger M, Schneider C, Koehler J. Energy savings and increased electric vehicle range through improved battery thermal management. Applied Thermal Engineering. 2016;101:647-56.

[159] Situ W, Zhang G, Li X, Yang X, Wei C, Rao M, et al. A thermal management system for rectangular LiFePO4 battery module using novel double copper mesh-enhanced phase change material plates. Energy. 2017;141:613-23.

[160] Wu W, Wu W, Wang S. Thermal optimization of composite PCM based large-format lithium-ion battery modules under extreme operating conditions. Energy Conversion and Management. 2017;153:22-33.

[161] Mortazavi B, Yang H, Mohebbi F, Cuniberti G, Rabczuk T. Graphene or h-BN paraffin composite structures for the thermal management of Li-ion batteries: A multiscale investigation. Applied Energy. 2017;202:323-34.

[162] Putra N, Ariantara B, Pamungkas RA. Experimental investigation on performance of lithium-ion battery thermal management system using flat plate loop heat pipe for electric vehicle application. Applied Thermal Engineering. 2016;99:784-9.

[163] Hussain A, Tso CY, Chao CYH. Experimental investigation of a passive thermal management system for high-powered lithium ion batteries using nickel foam-paraffin composite. Energy. 2016;115:209-18.

[164] Xie J, Ge Z, Zang M, Wang S. Structural optimization of lithium-ion battery pack with forced air cooling system. Applied Thermal Engineering. 2017;126:583-93.

[165] Xu J, Lan C, Qiao Y, Ma Y. Prevent thermal runaway of lithium-ion batteries with minichannel cooling. Applied Thermal Engineering. 2017;110:883-90.

[166] Gaultois M. From trash to treasure: Making electricity from waste heat. In: Williams L, editor. The Global Scientist2014.

[167] Thielmann J. Thermoelectric Cooling Technology. Will Peltier Modules Supersede the Compressor. 2013.

[168] Corporation T. Thermoelectric Cooling & Heating. 2017.

[169] Corporation F-N. Peltier Device: A Single Device Used for Cooling and Heating. WordPress.com2015.

[170] Alaoui C, Salameh ZM. A novel thermal management for electric and hybrid vehicles. IEEE transactions on vehicular technology. 2005;54:468-76.

[171] Cosnier M, Fraisse G, Luo L. An experimental and numerical study of a thermoelectric air-cooling and air-heating system. International Journal of Refrigeration. 2008;31:1051-62.

[172] Miranda A, Chen T, Hong C. Feasibility study of a green energy powered thermoelectric chip based air conditioner for electric vehicles. Energy. 2013;59:633-41.

[173] Suh I-S, Cho H, Lee M. Feasibility study on thermoelectric device to energy storage system of an electric vehicle. Energy. 2014;76:436-44.

[174] Rowe D, Goldsmid H. A new upper limit to the thermoelectric figure-of-merit. Thermoelectrics Handbook: Macro to Nano: CRC Press; 2005. p. 10-1--.

[175] Bell LE, LaGrandeur J, Davis S. Battery thermal management system including thermoelectric assemblies in thermal communication with a battery. Google Patents; 2015.

[176] Verma SS. Eco-friendly alternative refrigeration systems. Resonance. 2001;6:63-7.

[177] Tassou SA, Lewis JS, Ge YT, Hadawey A, Chaer I. A review of emerging technologies for food refrigeration applications. Appl Therm Eng2010. p. 263-76.

[178] Tijani MEH, Zeegers JCH, de Waele ATAM. Construction and performance of a thermoacoustic refrigerator. Cryogenics. 2002;42:59-66.

[179] Garrett SL, Hofler TJ. Thermoacoustic refrigeration. 1991.

[180] Paek I, Braun JE, Mongeau L. Evaluation of standing-wave thermoacoustic cycles for cooling applications. International Journal of Refrigeration. 2007;30:1059-71.

[181] Chrysler GM, Vader DT. Electronics package with improved thermal management by thermoacoustic heat pumping. Google Patents; 1994.

[182] Zink F, Vipperman JS, Schaefer LA. Environmental motivation to switch to thermoacoustic refrigeration. Applied Thermal Engineering. 2010;30:119-26.

[183] Pecharsky VK, Gschneidner Jr KA. Magnetocaloric effect and magnetic refrigeration. Journal of Magnetism and Magnetic Materials. 1999;200:44-56.

[184] Cremades E, Gómez-Coca S, Aravena D, Alvarez S, Ruiz E. Theoretical study of exchange coupling in 3d-Gd complexes: large magnetocaloric effect systems. Journal of the American Chemical Society. 2012;134:10532-42.

[185] Verma S. Eco-friendly alternative refrigeration systems. Resonance. 2001;6:57-67.

[186] Romero Gómez J, Ferreiro Garcia R, De Miguel Catoira A, Romero Gómez M. Magnetocaloric effect: A review of the thermodynamic cycles in magnetic refrigeration. Renewable and Sustainable Energy Reviews. 2013;17:74-82.

[187] Jeong S. AMR (Active Magnetic Regenerative) refrigeration for low temperature. Cryogenics. 2014;62:193-201.

[188] Debnath JC. Novel magnetocaloric materials and room temperature magnetic refrigeration. 2011.

[189] Barclay JA, Steyert WA. Active magnetic regenerator. Google Patents; 1982.

[190] Kitanovski A, Tušek J, Tomc U, Plaznik U, Ožbolt M, Poredoš A. Active Magnetic Regeneration. Magnetocaloric Energy Conversion: Springer; 2015. p. 97-166.

[191] Yu BF, Gao Q, Zhang B, Meng XZ, Chen Z. Review on research of room temperature magnetic refrigeration. International Journal of Refrigeration. 2003;26:622-36.

[192] Zhong XC, Tang PF, Liu ZW, Zeng DC, Zheng ZG, Yu HY, et al. Magnetic properties and large magnetocaloric effect in Gd–Ni amorphous ribbons for magnetic refrigeration applications in intermediate temperature range. Journal of Alloys and Compounds. 2011;509:6889-92.

[193] Applications C. Magnetic Refrigeration System - The Benefits. 2017.

[194] Applications C. Cooltech Applications Launches the First Magnetic Cooling System for Commercial Refrigeration. Business Wire, Inc.; 2016.

[195] Drake SJ, Martin M, Wetz DA, Ostanek JK, Miller SP, Heinzel JM, et al. Heat generation rate measurement in a Li-ion cell at large C-rates through temperature and heat flux measurements. Journal of Power Sources. 2015;285:266-73.

[196] Parise RJ. Quick charge battery with thermal management. Google Patents; 2003.

[197] Bandhauer TM, Garimella S. Passive, internal thermal management system for batteries using microscale liquid–vapor phase change. Applied Thermal Engineering. 2013;61:756-69.

[198] Mohammadian SK, He Y-L, Zhang Y. Internal cooling of a lithium-ion battery using electrolyte as coolant through microchannels embedded inside the electrodes. Journal of Power Sources. 2015;293:458-66.

[199] Shah K, McKee C, Chalise D, Jain A. Experimental and numerical investigation of core cooling of Li-ion cells using heat pipes. Energy. 2016;113:852-60.

[200] Rao Z, Wang S. A review of power battery thermal energy management. Renewable and Sustainable Energy Reviews. 2011;15:4554-71.

[201] Arora S, Kapoor A, Shen W. A novel thermal management system for improving discharge/charge performance of Li-ion battery packs under abuse. Journal of Power Sources. 2018;378:759-75.

[202] Pesaran AA, Burch S, Keyser M, Institut Mech Engineers; Institut Mech E. An approach for designing thermal management systems for electric and hybrid vehicle battery packs1999.